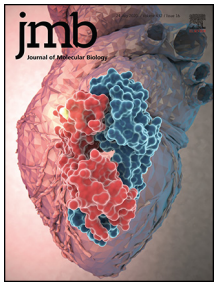

Local c-di-GMP Signaling in the Control of Synthesis of the *E. coli* Biofilm Exopolysaccharide pEtN-Cellulose

Anja M. Richter[1,4], Alexandra Possling[1], Nadezhda Malysheva[2,3], Kaveh P. Yousef[2], Susanne Herbst[1], Max von Kleist[2,3] and Regine Hengge[1]

*1 - **Institute of Biology/Microbiology,** Humboldt-Universität zu Berlin, 10115 Berlin, Germany*
*2 - **Department of Mathematics and Computer Science,** Freie Universität Berlin, 14195 Berlin, Germany*
*3 - **MF1 Bioinformatics,** Robert-Koch-Institut, 13353 Berlin, Germany*
*4 - **Department of Materials and the Environment,** Bundesanstalt für Materialforschung und -Prüfung, 12205 Berlin, Germany*

***Correspondence to Regine Hengge:** Institut für Biologie/Mikrobiologie, Humboldt-Universität zu Berlin, Philippstr. 13 – Haus 22, 10115 Berlin, Germany. regine.hengge@hu-berlin.de*
https://doi.org/10.1016/j.jmb.2020.06.006
Edited by Urs Jenal

Abstract

In many bacteria, the biofilm-promoting second messenger c-di-GMP is produced and degraded by multiple diguanylate cyclases (DGC) and phosphodiesterases (PDE), respectively. High target specificity of some of these enzymes has led to theoretical concepts of "local" c-di-GMP signaling. In *Escherichia coli* K-12, which has 12 DGCs and 13 PDEs, a single DGC, DgcC, is specifically required for the biosynthesis of the biofilm exopolysaccharide pEtN-cellulose without affecting the cellular c-di-GMP pool, but the mechanistic basis of this target specificity has remained obscure. DGC activity of membrane-associated DgcC, which is demonstrated *in vitro* in nanodiscs, is shown to be necessary and sufficient to specifically activate cellulose biosynthesis *in vivo*. DgcC and a particular PDE, PdeK (encoded right next to the cellulose operon), directly interact with cellulose synthase subunit BcsB and with each other, thus establishing physical proximity between cellulose synthase and a local source and sink of c-di-GMP. This arrangement provides a localized, yet open source of c-di-GMP right next to cellulose synthase subunit BcsA, which needs allosteric activation by c-di-GMP. Through mathematical modeling and simulation, we demonstrate that BcsA binding from the low cytosolic c-di-GMP pool in *E. coli* is negligible, whereas a single c-di-GMP molecule that is produced and released in direct proximity to cellulose synthase increases the probability of c-di-GMP binding to BcsA several hundred-fold. This local c-di-GMP signaling could provide a blueprint for target-specific second messenger signaling also in other bacteria where multiple second messenger producing and degrading enzymes exist.

Introduction

In many bacterial species, the ubiquitous bacterial second messenger bis-(3′–5′)-cyclic diguanosine monophosphate (c-di-GMP) is produced and degraded by multiple diguanylate cyclases (DGC) and specific phosphodiesterases (PDE), respectively. Surprisingly, some of these enzymes generate distinct and highly specific regulatory outputs, even though they all control the same cytoplasmic second messenger [1–4]. What is the basis of such specificity on a background of sometimes dozens of other DGCs and PDEs? In other words, how can c-di-GMP produced by a single distinct DGC be essential for, e.g., the expression of a particular gene or the biosynthesis of a specific exopolysaccharide during biofilm formation, while other DGCs of that species, which are expressed and active at the same time, do not contribute to this specific function? As suggested theoretically already 10 years ago [2], such high target specificity could reflect local c-di-GMP signaling based on specific direct interactions in c-di-GMP signaling modules that comprise a DGC and/or PDE with a specific c-di-GMP-binding effector/target system in a multi-protein complex.

Escherichia coli K-12 is an excellent model organism to systematically address the question of output specificity of distinct DGCs and PDEs [5]. Its genome contains genes for 12 DGCs (with this activity residing in GGDEF domains), 13 PDEs (with EAL domains providing PDE activity) as well as four "degenerate" GGDEF/EAL domain proteins [6,7], the latter with non-enzymatic functions relying on direct macromolecular interactions [8–10]. Nearly all of these GGDEF/EAL domain proteins are expressed and most of the DGCs are active when *E. coli* cells enter into stationary phase [11,12]. Moreover, several c-di-GMP-controlled targets are known for *E. coli*, with the underlying effector mechanisms having been analyzed at the molecular level. Target mechanisms include c-di-GMP-stimulated transcription of the gene for the biofilm matrix regulator CsgD [13], biosynthesis of the biofilm matrix exopolysaccharides phosphoethanolamine (pEtN)-cellulose [14–16] and poly-*N*-acetyl-glucose (poly-GlcNAc or PGA) [17] as well as an inhibition of flagellum rotation [18–21].

c-di-GMP-mediated control of transcriptional initiation at the promoter of *csgD*, encoding the activator of biosynthesis of the biofilm matrix components pEtN-cellulose and curli in *E. coli*, has become a paradigm of local c-di-GMP signaling. Here, the "trigger PDE" PdeR directly interacts with and thereby inhibits both DgcM and the MerR-like transcription factor MlrA, and thereby prevents *csgD* transcription [13]. During entry into stationary phase, it is specifically DgcE, which is both induced and activated and can also interact with PdeR [12,22], that generates c-di-GMP to "trigger" PdeR to release DgcM and MlrA [13,23]. As a consequence, DgcM now also produces c-di-GMP and at the same time acts as a transcriptional co-activator for *csgD* in a complex with MlrA [13]. Knockout mutations in *dgcE*, *pdeR* or *dgcM* do not alter overall cellular c-di-GMP levels, although they have drastic effects on biofilm matrix production [12,13,18,24]. Moreover, these components constitute the core of a network or "supermodule" of several interacting DGCs and PDEs, in which protein–protein interactions assume direct regulatory roles [12,23].

In this study, we present a mechanistically alternative type of local c-di-GMP signaling. It has long been known that the DGC AdrA (in *Salmonella*) and its *E. coli* counterpart DgcC (formerly YaiC) are specifically required to produce cellulose [25,26]. The membrane-integral BcsAB complex, which couples glucosyltransferase activity with the co-synthetic secretion of cellulose, is allosterically activated by c-di-GMP binding to the PilZ domain of the BcsA subunit [27]. Upon its emergence into the periplasm, cellulose is modified by the attachment of pEtN groups, a process that is catalyzed by BcsG and controlled by transmembrane c-di-GMP signaling *via* BcsE and BcsF [16]. Here, we demonstrate that *E. coli* core cellulose synthase BcsAB directly interacts with DgcC and PdeK. In contrast to the *regulatory* interactions within the DgcE/PdeR/DgcM/MlrA module described above, protein–protein contacts in the DgcC/PdeK/BcsB/BcsA module exert a *scaffolding* function, i.e. generate signaling specificity by localizing a specific source (DgcC) and sink (PdeK) of c-di-GMP in the immediate vicinity of the c-di-GMP-binding BcsA subunit of cellulose synthase. Using mathematical modeling, we show that the close co-localization of a specific source and effector binding site for c-di-GMP strongly increases the c-di-GMP binding probability for the effector component and enables robust and accurate signaling without the need for further compartmentalization.

Results

DgcC and PdeK: roles in cellulose biosynthesis and enzymatic activities *in vitro*

Production of an extracellular polymeric matrix is the essential hallmark of a bacterial biofilm [28,29]. In *E. coli* macrocolony biofilms that grow for extended times on agar plates, the extracellular matrix consisting of amyloid fibers of curli proteins and the exopolysaccharide pEtN-cellulose determines stability, cohesion and elasticity of the biofilm, i.e. tissue-like properties that allow macrocolonies to buckle up and fold into complex morphological patterns. The actual composition of the extracellular matrix, just amyloid curli fibers or pEtN-cellulose or a combination of both, determines the intricate shape of macrocolonies (Figure 1), i.e. colony morphology is a convenient phenotype for genetic studies of matrix production and regulation [30–32].

Putative effects on pEtN-cellulose and/or curli biosynthesis of any of the knockout mutations in the genes encoding the 29 GGDEF/EAL domain protein of *E. coli* K-12 are therefore revealed by altered macrocolony morphology [12]. Of all 12 DGC knockouts, only Δ*dgcC* generates a specific phenotype resembling that of a cellulose-free *ΔbcsA* mutant: (i) a pattern of concentric rings indicating high curli production only on salt-free LB/Congo red (CR) agar plates (Figure 1); (ii) flat colonies with CR staining reflecting the presence of residual curli fibers on Yesca/CR medium, where matrix production is generally less pronounced (Figure 1); and (iii) reduced staining with calcofluor (Figure S1). Eliminating DgcC has no effect on the expression of the curli operon (Figure S2), even though synthesis of both curli and pEtN-cellulose depends on the DGCs DgcE and DgcM to express CsgD at a higher level of the hierarchical control network [12,33]. Thus, DgcC plays a highly specific and potentially local role in the c-di-GMP control of cellulose synthase activity [12].

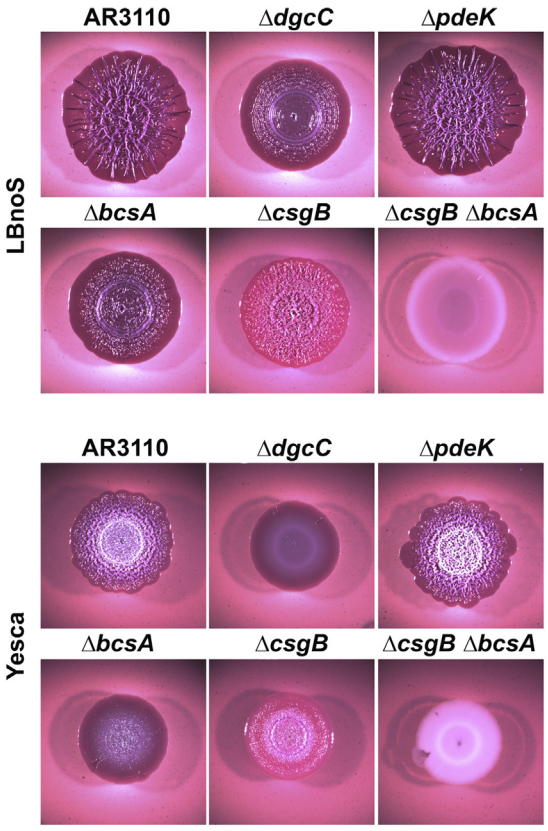

Figure 1. Contributions of pEtN-cellulose and curli fibers as well as DgcC and PdeK to the morphology of macrocolony biofilms of *E. coli* K-12. Macrocolonies of *E. coli* K-12 strain AR3110 and its derivatives with deletion mutations in genes encoding DgcC, PdeK, cellulose synthase subunit BcsB and/or curli subunit CsgB were grown for 5 days at 28 °C either on salt-free LB agar plates (top rows) or Yesca/CR agar plates (bottom rows) supplemented with CR. The *E. coli* K-12 strain AR3110, which produces both amyloid curli fibers and pEtN-cellulose [30], grows in large flat macrocolonies that generate a combination of long and high ridges and smaller wrinkles. By contrast, a pEtN-cellulose-deficient derivative (*ΔbcsA*) generates a pattern of concentric rings reflecting deep breaks of its brittle non-elastic curli-only matrix; a curli-negative mutant (*ΔcsgB*), which produces cellulose as the only matrix component, grows in tiny intertwined wrinkles reflecting high elasticity but little large-scale stability of the matrix [30].

In addition, the hitherto uncharacterized membrane-associated PDE PdeK was included in our analysis of c-di-GMP control of cellulose production. In many bacterial species, the *pdeK* gene is located right next to the major cellulose operon (*yhjR-bcsQABZC*) suggesting a potential functional linkage with cellulose biosynthesis. The *ΔpdeK* mutant seemed to generate slightly more small wrinkles, especially when grown on Yesca/CR agar plates (Figure 1), suggesting that PdeK could possibly play a negative role in cellulose biosynthesis.

The DgcC amino acid sequence includes a catalytic center motif (the "A-site" or GGDEF) and an intact "I-site" motif (RSGD; conferring potential product inhibition) as characteristic for DGCs [34] and also the EAL domain of PdeK contains the amino acids crucially involved in PDE activity [35–38]. Nevertheless, we wanted to show their enzymatic activities directly *in vitro*, which is not trivial since both proteins are membrane-integrated. DgcC consists of a MASE2 domain with six transmembrane (TM) regions, followed by the GGDEF domain [39]. PdeK features an N-terminal GAPES3 domain (with two transmembrane regions flanking the periplasmic region) followed by a HAMP linker domain, a degenerate GGDEF ($GGDEF^{deg}$) and the intact EAL domain [6].

When cloned and purified alone, the soluble GGDEF domain of DgcC did not exhibit any DGC activity, which is consistent with the isolated GGDEF domain being unable to dimerize *in vivo* [12]. By contrast, the membrane-inserted MASE2 domain alone showed *in vivo* dimerization in a bacterial two-hybrid system (Figure 2(a)). This two-hybrid system is based on the reconstitution of adenylate cyclase (AC) activity from its separated T18 and T25 domains, which allows to assay membrane-integral proteins [40]. Also in this system, the inability of the GGDEF domain to dimerize on its own was confirmed (Figure 2(a)). Dimer formation by the MASE2 domain explains its activating role for DgcC since dimerizing N-terminal domains can assist the dimerization of the GGDEF domain, which is a prerequisite for enzymatic activity of DGCs [42].

In order to demonstrate this DGC activity *in vitro*, we therefore purified the complete DgcC protein (with a C-terminal Strep tag) for reconstitution in a quasi-native membrane environment. For the latter, we chose the nanodisc system, i.e. self-assembled discoidal phospholipid bilayers stabilized by a thread-like membrane scaffold protein (MSP; derived from human apolipoprotein A-I), which wraps around the phospholipid bilayer that can incorporate a transmembrane protein or protein complexes [43–45]. In order to accommodate a DgcC dimer per nanodisc, a relatively large MSP was chosen (MSP1E3D1). Once reconstituted and purified (by affinity chromatography *via* the Strep tag on DgcC), the DgcC-containing nanodiscs were soluble and DGC activity could indeed be measured by the standard enzyme assay (Figure 2(b)). DgcC showed clear activity in the presence of Mn^{++}, which is in contrast to the widely used soluble standard DGC PleD* [42], which is less demanding with respect to cations and can operate in the presence of Mg^{++}, Mn^{++} or Ca^{++} (Figure S3). In addition, DgcC showed only weak inhibition by high concentrations of its product c-di-GMP (Figure 2(b)), which in PleD and many other DGCs is mediated by allosteric regulation *via* the I-site [34]. Finally, DgcC exhibited a K_m

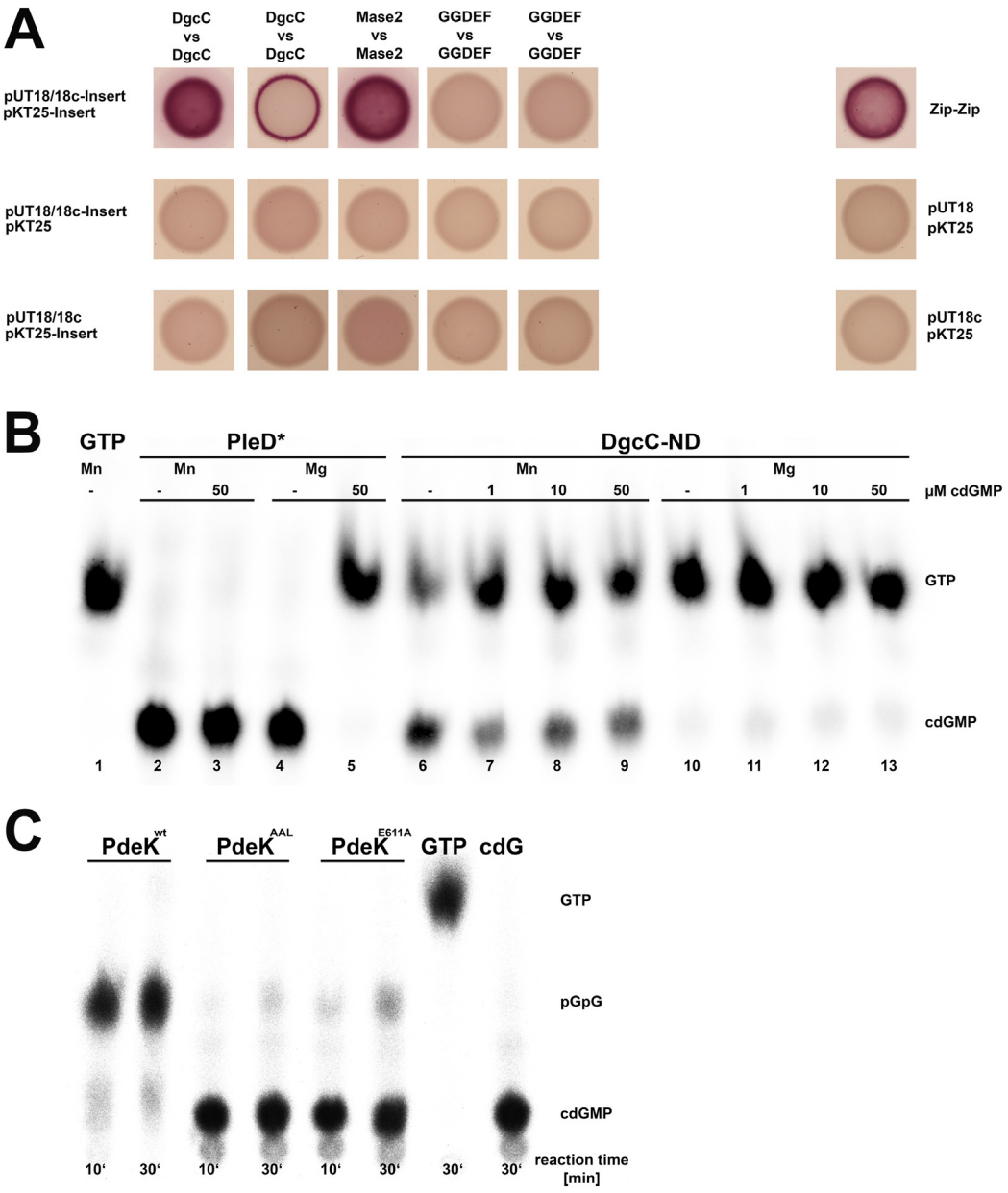

Figure 2. Dimerization of DgcC and *in vitro* enzymatic activities of full-size DgcC reconstituted in nanodiscs and of the cytoplasmic moiety of PdeK. (a) *In vivo* dimerization of DgcC and its isolated MASE2 or GGDEF domains was tested using a bacterial two-hybrid system. The assay is based on the reconstitution of AC from its T18 and T25 domains [40], which were fused to DgcC or its domains as indicated. Dimerization of the latter ones allows the cAMP/CRP-dependent utilization of lactose as a C-source by an *E. coli Δcya* strain (resulting in red color on MacConkey plates). In two similarly labeled spots, the upper partner was cloned into pUT18 in one spot and into pUT18c in the other spot (i.e. the indicated protein, e.g. DgcC, was inserted either at the N terminus or C terminus of the AC fragment T18, respectively). The MASE2 domain alone could be stably cloned into pUT18 only (generating MASE2::T18). The two bottom rows show the negative controls, where only one of the two cotransformed plasmids contained the indicated cloned insert. As a positive control, the leucin zipper part of the yeast GCN4 protein was used. (b) In order to test membrane-bound DgcC for DGC activity, 3.5 µM purified DgcC-Strep incorporated into nanodiscs was assayed using 82.5 nM [P^{33}]-GTP in the presence of either Mn^{++} or Mg^{++}, with unlabeled c-di-GMP added as indicated (to test for I-site-mediated inhibition). Purified PleD* (a mutationally activated DGC from *Caulobacter crescentus* [41]) served as a positive control. Samples were taken after a 60-min incubation and analyzed by thin-layer chromatography. (c) The purified cytoplasmic part (amino acids 148–649, constituting the $GGDEF^{deg}$ and EAL domains) of PdeK and the indicated mutant variants of PdeK (AAL, which stands for the E431A/V432A exchanges, and E611A) were assayed for PDE activity using 1 µM Strep-tagged truncated proteins and 82.5 nM [P^{33}]-c-di-GMP. Samples were taken after 10 and 30 min and further analyzed as for the DGC assays.

for GTP of 2 μM (Figure S4), indicating that it operates at substrate saturation *in vivo*, since GTP is present at a cellular concentration of about 1 mM [46]. To our knowledge, these experiments with DgcC also represent the first report of a reconstitution of an enzymatically active full-size membrane-integral GGDEF domain protein in nanodiscs, which provide an excellent tool to study the activities and regulation of membrane-inserted proteins, since protein regions on both sides of the membrane are fully accessible.

PDE activity of PdeK could be demonstrated with the purified soluble cytoplasmic parts alone (PdeK^{wt}, with "wt" referring to the intact sequence of its EAL domain; Figure 2(c)). This cytoplasmic part of PdeK was highly active under standard conditions, with its activity depending on an intact EAL motif as well as the catalytic glutamic acid residue (E611 in the full-size protein). This not only established PdeK as an active PDE, but also indicates that its degenerate GGDEF domain does not inhibit its activity (at least in the absence of the extracytoplasmic domains). Thus, the membrane-integral/periplasmic domains of PdeK are not required for its PDE activity, but may modulate this activity in response to unknown signals and/or have a function in specific localization.

DgcC directly interacts with cellulose synthase and PdeK

Local and highly specific c-di-GMP-mediated activation of a particular target can be expected to involve direct interactions between the specific DGC and the effector/target system. To test this hypothesis for DgcC and cellulose synthase, we used *E. coli* strain 1094 *bcsA*$^{HA\text{-}Flag}$ 2 K7 [47], which constitutively expresses, from its chromosome, the divergent operons *yhjR-bcsQABZC* (for cellulose synthesis) and *bcsEFG* (for pEtN modification of cellulose). BcsA expressed in this strain carries a C-terminal HA-Flag tag (gene designated as *bcsA** in Figure 3), which allows to pull down the core cellulose synthase complex with additional proteins bound in affinity chromatography experiments using FlagM2 resin [47]. In this strain background, DgcC was expressed from a low copy number plasmid with a His6 tag (gene designated as *dgcC*$^{\#}$ in Figure 3), which allows its detection by immunoblot analysis. As visualized by anti-Flag antibodies by immunoblot detection (Figure 3), BcsA was retained and eluted from anti-FlagM2 resin and produced the characteristic band pattern previously observed by Krasteva *et al.* [47], with >250-kD BcsA/BcsB complexes, full-length BcsA and proteolytic BcsA fragments (Figure 3). When DgcC::His6 was coexpressed in the *bcsA** strain, it was indeed co-eluted from the anti-FlagM2 affinity chromatography matrix (Figure 3). This interaction was specific for BcsA and/or the Bcs complexes formed by BcsA, since DgcC::His6 produced in the Flag tag-free strain 1094 ("WT") was not retained by the anti-FlagM2 resin.

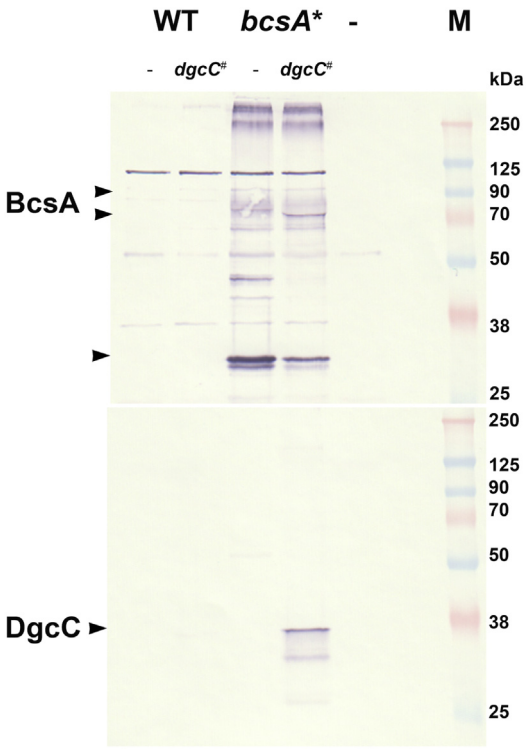

Figure 3. DgcC co-purifies with the cellulose synthase complex. DgcC::His6 was expressed from the low copy number vector pCAB18 either in *E. coli* strains 1094 (WT; first two lanes) or 1094 *bcsA*$^{HA\text{-}Flag}$ 2 K7, with the latter producing BcsA with a HA-Flag tag (from the chromosomal *bcsA** allele; third and fourth lane) [47]. Affinity chromatography was performed with the indicated cellular extracts on anti-FlagM2 resin, which specifically binds the Flag tag of BcsA. Eluates were analyzed in parallel on two identical SDS polyacrylamide gels, followed by visualization of BcsA (including >250 kD BcsA complexes with other proteins as well as full-size BcsA and BcsA degradation products indicated by arrow heads) and DgcC by immunoblotting using anti-Flag (upper panel) and anti-His6 antibodies (lower panel), respectively. The last three lanes contained a similarly treated control sample without cellular extracts and the molecular mass marker (with an empty lane between the two).

Direct protein interactions were further analyzed *in vivo* using the bacterial two-hybrid system already introduced above [40]. The AC domains were linked to the N- and C-termini of BcsA, whereas at BcsB, a fusion can only be at the C terminus since the large N-terminal part of the protein is localized to the periplasm. As expected from the cellulose synthase core structure [48], the two-hybrid assays reflected complex formation between BcsA and BcsB (Figure 4). Furthermore, the data revealed interaction of DgcC with BcsB, which was specific since no interaction with BcsA could be detected. In addition, DgcC interacted with PdeK (note that due to potential steric hindrance, in particular with membrane-inserted proteins, reconstitution of AC is not necessarily always fully reciprocal in vector-swaps).

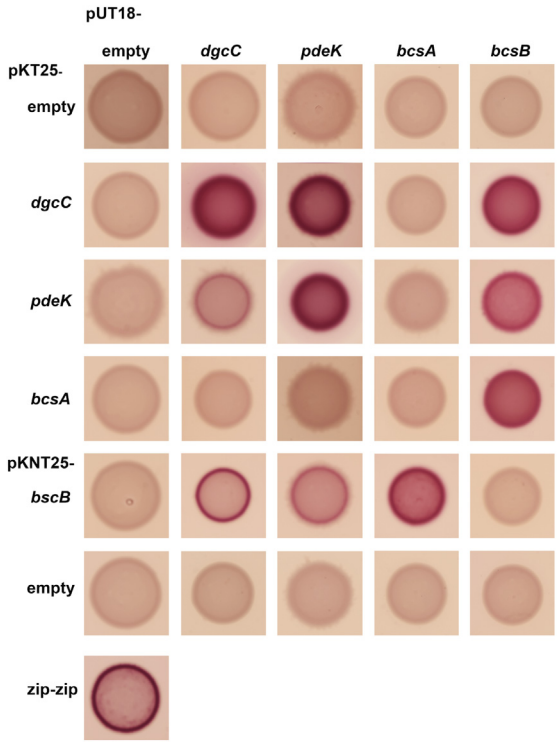

Figure 4. DgcC interacts *in vivo* with cellulose synthase subunit BcsB and PdeK. Interactions of the indicated proteins *in vivo* were tested using the bacterial two-hybrid system based on the reconstution of AC [40] described above in the legend to Figure 2. Interactions between DgcC, BcsB and PdeK were shown with two-hybrid constructs that produced hybrid proteins linking T18/T25 AC domains and the indicated full-size proteins.

Also PdeK showed interaction with BcsB and the potential to dimerize (Figure 4), with dimerization being expected for PDEs [49,50]. These results indicate that DgcC can bind to the cellulose synthase complex *via* the BcsB subunit and that PdeK may also dock to this complex by interacting both with DgcC and BcsB.

These interactions were further characterized using isolated domains or internal deletion variants of DgcC and PdeK in two-hybrid analyses. Only the membrane-integral MASE2 domain of DgcC, but not its cytoplasmic GGDEF domain, interacted with BcsB (Figure 5), consistent with BcsB being composed of a transmembrane anchor and a large periplasmic domain [48]. The interaction between PdeK and BcsB was found to require neither the cytoplasmic part of PdeK, comprising the GGDEF^{deg} and EAL domains, nor the periplasmic loop domain (Figure 5), i.e. this interaction relies on the transmembrane regions of PdeK. Finally, the interaction between DgcC and PdeK did also not involve their respective cytoplasmic domains, but required the membrane-integral MASE2 domain of DgcC and the periplasmic loop domain of PdeK (Figure 5). This is consistent with a previous report, where the soluble cytoplasmic parts of DgcC and PdeK did not show interaction in the alternative Bacterio-Match® II two-hybrid system, which is suitable for soluble cytoplasmic proteins or domains only [12]. Taken together, the interactions of BcsB with either DgcC or PdeK occur mainly within the membrane, whereas PdeK seems to contact DgcC's MASE2 domain mainly on the outer side of the membrane *via* the periplasmic loop of its GAPES3 domain.

In conclusion, these *in vitro* and *in vivo* interaction studies show that DgcC and PdeK not only interact with each other, but that both can interact with cellulose synthase *via* their membrane-integral domains contacting the BcsB subunit. Overall, these data suggest that a direct source (DgcC) and sink (PdeK) for c-di-GMP can be established in the immediate vicinity of core cellulose synthase and may thus be part of the larger cellulose synthase complex.

Molecular functions of DgcC and PdeK in the local c-di-GMP control of cellulose synthase activity

Is the control of c-di-GMP production and decay in the direct neighborhood of cellulose synthase the only function of DgcC and PdeK in the complex with BcsA/BcsB or could their protein–protein interactions within this complex also play direct activating or inhibitory roles? The latter principle is exemplified by the bifunctional trigger PDE PdeR, which directly inhibits its two partner proteins DgcM and MlrA, with its binding and degradation of c-di-GMP modulating this inhibition. Importantly, regulatory impact and enzymatic activity of PdeR can be genetically separated, i.e. an enzymatically inactive PdeR variant is still a regulator, which behaves as a "c-di-GMP-blind superinhibitor" [13].

In order to test, whether DgcC not only controls c-di-GMP but possibly also affects cellulose synthase activity directly by its interaction with BcsB, we compared the effects of a full *ΔdgcC* deletion with just an active site point mutation (GGAAF, also introduced in the chromosomal copy of *dgcC*). Similar expression of wild-type DgcC and DgcC^{GGAAF} was shown by immunoblot experiments with derivatives carrying C-terminal Flag tags (Figure S6). Thus, introducing the GGAAF mutation eliminates DGC activity, but does not significantly affect the stoichiometry between DgcC and the Bcs complex. Despite normal expression of DgcC^{GGAAF}, the *dgcC*^{GGAAF} mutant showed the same phenotype as the *ΔdgcC* complete deletion strain, both with respect to macrocolony morphology on salt-free LB and Yesca agar as well as to calcofluor binding (Figure 6(a), left panel). These identical mutant phenotypes of the active center point mutation and the complete deletion mutation strongly indicate that DgcC relies specifically and exclusively on its enzymatic activity for controlling cellulose biosynthesis. Following

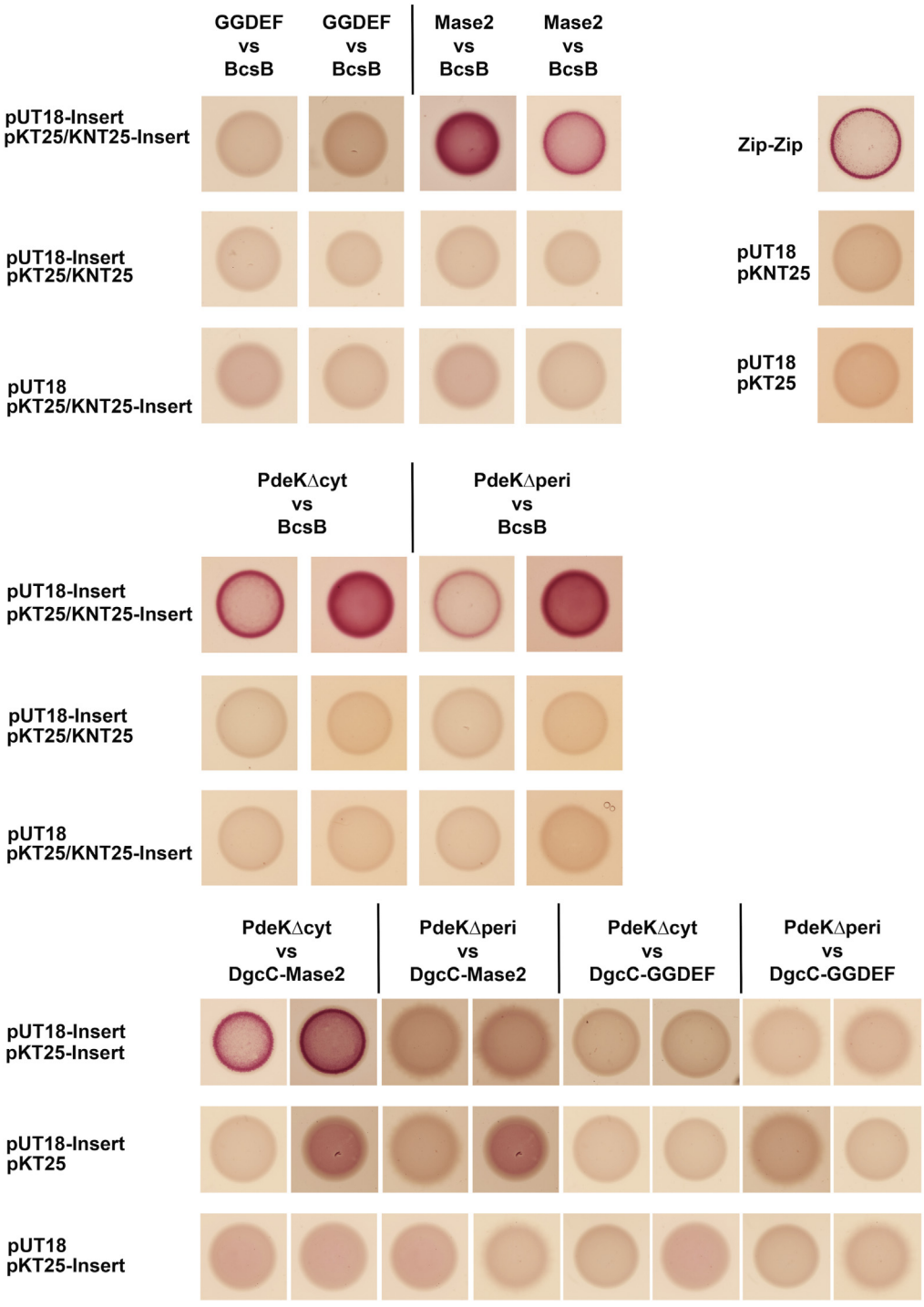

Figure 5. Interactions between BcsB, DgcC and PdeK occur in the extracytoplasmic domains of these proteins. Specific domains or parts of DgcC and PdeK were probed for *in vivo* interactions with BcsB or each other by using the bacterial two-hybrid system based on the reconstution of AC [40] described above in the legend to Figure 2. The T18/T25 two-hybrid constructs contained the isolated MASE2 or GGDEF domains of DgcC and PdeK variants with internal domain deletions (*Δcyt*, absence of the entire cytoplasmic part, i.e. both the GGDEF^{deg} and EAL domains; *Δperi*, precise deletion of amino acids 26–136 eliminated the periplasmic loop of the GAPES3 domain of PdeK).

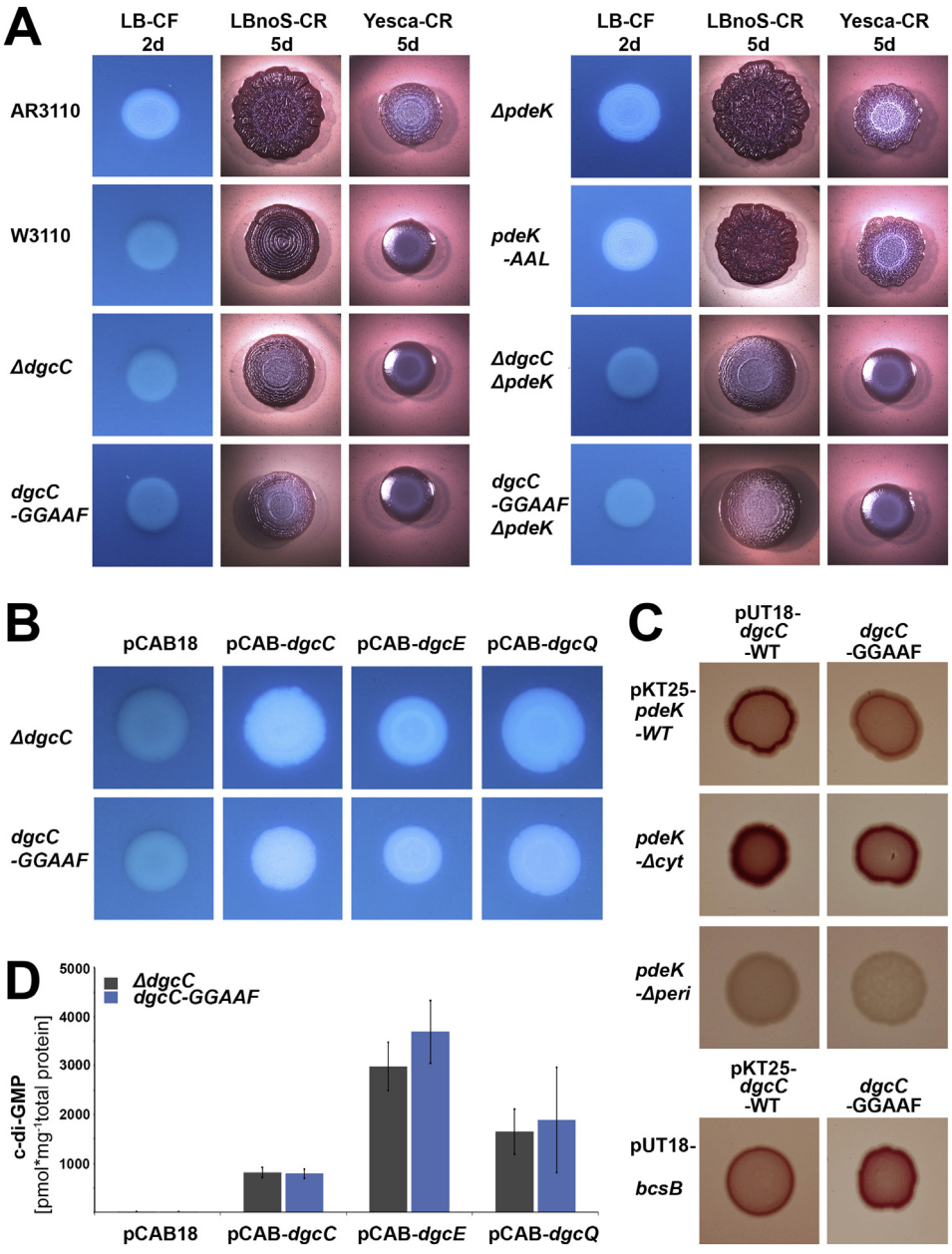

Figure 6. In the control of cellulose synthase, DgcC and PdeK act as a c-di-GMP source and sink, respectively, in an open non-compartmentalized system. (a) In order to test whether DgcC and PdeK affect cellulose biosynthesis by their enzymatic activities only and not by regulatory protein–protein interactions, calcofluor binding and macrocolony morphologies were compared for derivatives of strain AR3110 carrying (i) full deletions (*ΔdgcC*, *ΔpdeK*) and/or (ii) point mutations in *dgcC* (GGAAF) or *pdeK* (AAL) that allow for normal expression of just enzymatically inactive DgcC and PdeK. Macrocolonies were grown for 2 days on salt-free LB (calcofluor binding visualized by UV irradiation) or 5 days on salt-free LB or Yesca agar (colony morphology images). The classical *E. coli* K-12 strain W3110 served as a cellulose-negative control (residual staining is due to calcofluor binding also to curli fibers) otherwise isogenic to the cellulose-proficient strain AR3110. (b) The DGCs DgcC, DgcE and DgcQ were expressed under the control of the leaky *tac* promoter from the low copy number plasmid pCAB18 in AR3110 derivatives carrying either a full deletion (*ΔdgcC*) or the $dgcC^{GGAAF}$ allele in the chromosome, from where $DgcC^{GGAAF}$ is expressed at wild-type levels. Macrocolonies were grown for 2 days on calcofluor-containing salt-free LB agar plates, and calcofluor binding was visualized by UV radiation. (c) Similar interaction of $DgcC^{GGAAF}$ and wild-type DgcC with PdeK and BcsB was shown by two-hybrid analysis using the same constructs as described in Figures 4 and 5. (d) Cellular c-di-GMP levels were determined for derivatives of *E. coli* K-12 strain AR3110 carrying the same chromosomal *dgcC* alleles and plasmids described in (b).

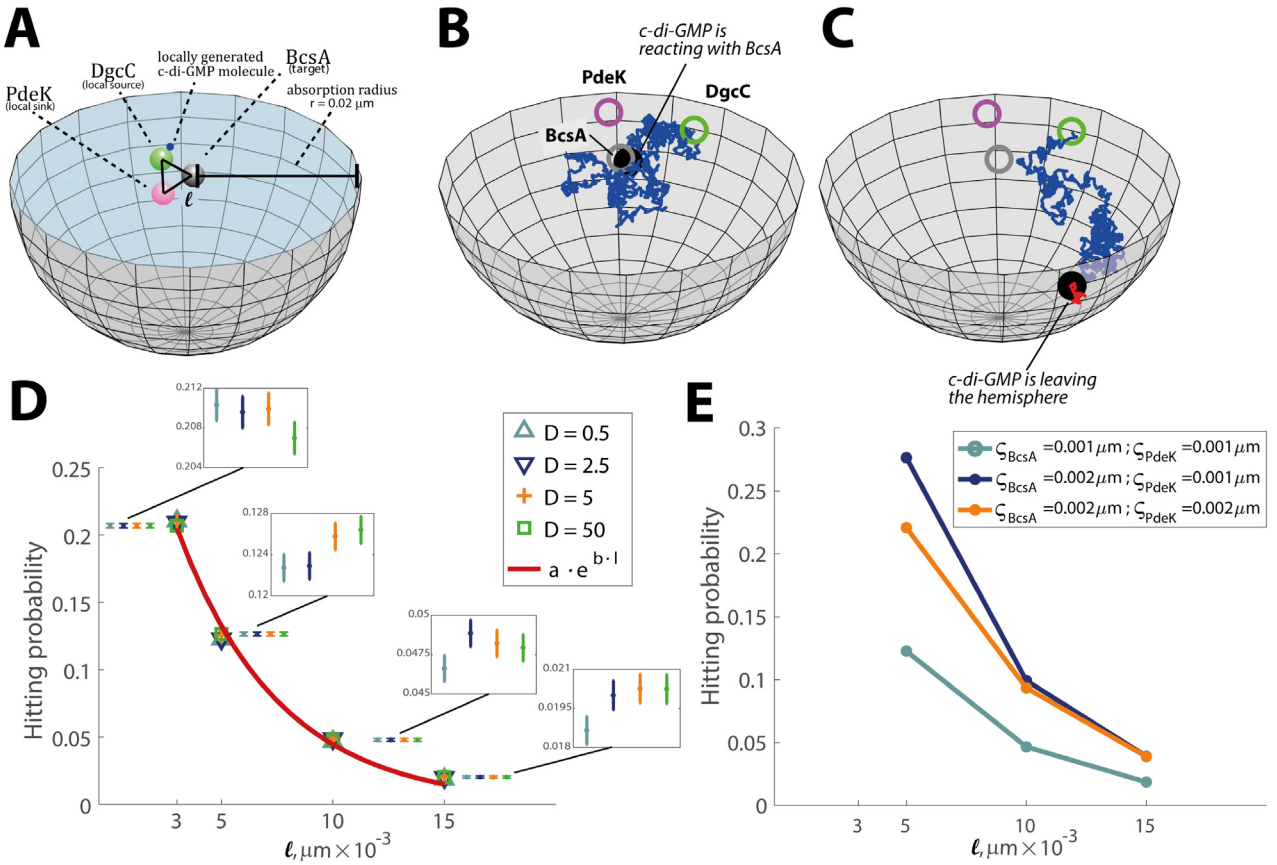

Figure 7. Mathematical modeling of local c-di-GMP signaling by BcsA, DgcC and PdeK interaction. (a) Setup of the modeled system. BcsA, DgcC and PdeK were placed in an equilateral triangle with side length *l* on the cell membrane. A hemisphere, centered around BcsA, with radius *r* = 0.02 μm defines an absorption radius; i.e. when c-di-GMP leaves this hemisphere, it is considered to be eliminated by a global sink (i.e. PdeH). (b) Trajectory (blue line) hitting BcsA. The solid black circle indicates the position of c-di-GMP when it enters the reaction radius of BcsA. (c) Trajectory before (blue line) and shortly after (red line) leaving the local hemisphere, after which it is unlikely to hit the local target. The solid black circle indicates the position of c-di-GMP when it leaves the hemisphere. Gray, green and magenta circles represent the reaction radii of BcsA, DgcC and PdeK, respectively. (d) Dependency of the hitting probability on the DgcC–BcsA–PdeK distance *l* and diffusion coefficient *D* for a reaction radius ρ = 0.001 μm. The red curve is an exponential function with fitted parameters *a* and *b* (see Supplementary Information) that depends on the DgcC-BcsA-PdeK distance *l*. Error bars represent 95% confidence interval for data presented on the left, calculated with Greenwood's formula. (e) Dependency of the hitting probability on the DgcC–BcsA–PdeK distance *l* and reaction radius ρ. A minimum distance (*l* = 5 nm) was chosen that exceeds all considered reaction radii.

Table 1. Modeling and simulation

Parameter	Explanation/assumption
BcsA–DgcC–PdeK distance *l*	The local system BcsA–DgcC–PdeK is located in a cell membrane (fixed). For simplicity, all three parts of this system (local target, c-di-GMP source and sink) were assumed to be equidistant from each other (i.e. to form an equilateral triangle), as shown in Figure 7(a).
Diffusion coefficient *D*	Olson *et al.* report an *in vivo* diffusion coefficient for cGMP (range, 1.4–5.*5* $\mu m^2\ s^{-1}$) [54]. Due to a larger molecular mass and size of c-di-GMP, as compared to cGMP, we also considered smaller parameters of *D*, starting with 0.5 $\mu m^2\ s^{-1}$. The diffusion coefficient reported by Zhou *et al.* for c-di-GMP/endo-S-c-di-GMP/2′-F-endo-S-c-di-GMP in aqueous solution (270–280 $\mu m^2\ s^{-1}$) is likely too large as it neglects cellular crowding effects [55]. When testing diffusion coefficients in the range (D = 0.5–50 $\mu m^2\ s^{-1}$), we found no dependency of the hitting probability on this parameter (Supplementary Information).
Reaction radius ρ	The reaction radius ρ describes a hypothetical sphere around the BcsA and the PdeK molecule determining its minimal distance to c-di-GMP required for a reaction, e.g. binding of c-di-GMP to the PilZ domain of BcsA. PdeK and BcsA [48,56] are both proteins, whose typical spherical radii is in the range of 0.001–0.005 μm [57]. Therefore, a conservative estimate (conservative in the sense that the reaction probability may be underestimated) of the reaction radius is 0.001 μm. Throughout this work, we test reaction radii in the range 0.001–0.002 μm.
Drift coefficient ∇	To test whether co-localization alone could explain local c-di-GMP control of cellulose synthase, we did not assume any energy acting on the diffusing c-di-GMP particle aside from random fluctuations. Therefore, the parameter ∇ in Eq. (1) was set to 0.
Cell volume	During entry into stationary phase within a macrocolony biofilm, cells are very short rods with a diameter of approx. 1 μm and a length of approx. 1.2–1.3 μm [30,31], i.e. an average cell volume of approx. 1 μm^3.
Absorption radius	We define the distance from the target (BcsA), which, when exceeded by c-di-GMP molecules, results in a negligible probability to hit the target (BcsA), as the "absorption radius." Thereby, c-di-GMP molecules leaving a hemisphere defined by the absorption radius are considered eliminated from the 'local pool'. The derivation of this parameter is described in the Supplementary Information.

the same logics, also a chromosomal *pdeK*^{AAL} mutant was generated and phenotypically compared to the full *ΔpdeK* deletion strain. Also in this case, macrocolony morphology on different media and calcofluor binding were similar (Figure 6(a), right panel), indicating that also PdeK affects cellulose biosynthesis *via* its enzymatic activity only. Moreover, in the absence of DgcC protein (*ΔdgcC*) or DgcC activity (*dgcC*^{GGAAF}), the additional deletion of *pdeK* generated no phenotype (Figure 6(a), right panel), indicating that PdeK specifically antagonizes DgcC as a local source of c-di-GMP in the control of cellulose production.

This local action of DgcC and PdeK raised the question, whether these two antagonistic enzymes together with the large cellulose synthase complex (actually an oligomer of the core BcsA/BcsB complex and the BcsG/BcsF components that install the pEtN modification [47]) may constitute a closed microcompartment in which c-di-GMP and its target, i.e. the PilZ domain of BcsA, would be isolated from the global cellular c-di-GMP pool controlled by other DGCs and PDEs. This possibility was tested using cross-complementation assays with other DGCs. DgcE was chosen as a well-characterized membrane-associated DGC [22], DgcQ as soluble cytoplasmic DGC. Low copy number plasmids expressing DgcC, DgcE or DgcQ were introduced into two different strains lacking DgcC activity: (i) the *ΔdgcC* mutant, in which the complete absence of DgcC would not allow the formation of a putative closed microcompartment, and (ii) the *dgcC*^{GGAAF} mutant, in which the enzymatically inactive DgcC^{GGAAF} protein was expressed at normal level (Figure S6) and can also interact with BcsB and PdeK (as shown by two-hybrid analysis; Figure 6(c)). If a closed microcompartment is formed by the Bcs complex and DgcC^{GGAAF}, it would not contain c-di-GMP and DgcC^{GGAAF} would be expected to act in a dominant-negative manner in cross-complementation assays with other DGCs even if the latter established high cellular c-di-GMP levels. However, we observed that the plasmid-encoded DGCs DgcE and DgcQ, as well as plasmid-encoded DgcC itself, fully cross-complemented the lack of DgcC activity not only in the *ΔdgcC* background, but also in the *dgcC*^{GGAAF} mutant (Figure 6(b)).

Thus, no matter whether DgcC is completely absent or is present but just inactive, cellulose synthase can be activated when the global cellular c-di-GMP pool is elevated (Figure 6(d)) by ectopic overexpression of other DGCs, which at wild-type expression levels control other targets (CsgD expression, motility) but do not contribute to controlling cellulose synthase [12,13,18,19,22]. This finding argues against the existence of a closed microcompartment with a separate local c-di-GMP pool serving specifically the c-di-GMP-binding PilZ domain of BcsA, and in favor of DgcC acting as a local, yet *open* c-di-GMP source right next to cellulose synthase.

Mathematical modeling of local c-di-GMP signaling at cellulose synthase

As a complementary approach to the experiments described above, we wanted to assess by mathematical modeling, whether co-localization alone of a local c-di-GMP source (DgcC) and sink (PdeK) next to cellulose synthase could be a mechanism to explain DgcC-specific c-di-GMP control of cellulose

synthase activity. In this local system, the BcsA subunit operates both as the c-di-GMP binding effector (*via* its PilZ domain) and as the target (its PilZ domain-controlled glucosyltransferase domain), but for simplicity, BcsA is just referred to as the "target" in the following. To test this hypothesis, we assumed that c-di-GMP is produced in proximity to its target BcsA, but not retained by any mechanism or micro-compartment as suggested by the cross-complementation experiments described in the previous section.

Mathematical modeling set-up

We modeled the free diffusion of c-di-GMP by the following stochastic differential equation [51]:

$$dX(t) = \nabla dt + \sqrt{2D} \bullet W(t) \quad (1)$$

where $dX(t) = (x_1,x_2,x_3)r$ is a vector describing the position of the particle in 3D space at time t. The function $W(t)$ is a three-dimensional standard Wiener process and D and ∇ are diffusion and drift coefficients, respectively. For simulation, we used an adaptive time step Euler–Maruyama method in analogy to [52], which we validated against the original method [53]. The model-setup is depicted in Figure 7(a) and all parameters and assumptions of the modeling are described in Table 1. Simulation was stopped if c-di-GMP entered the reaction radius ρ of BcsA or PdeK (Figure 7(b)) or if it left a particular radius around BcsA (Figure 7(c)), from where it is unlikely to return and bind BcsA (the absorption radius; details in the Supplementary Information). We then numerically simulated 10^4 trajectories and counted the number of trajectories where c-di-GMP entered the reaction radius ρ of its target BcsA, giving rise to the hitting probability (probability that c-di-GMP enters the reaction radius ρ of BcsA).

Signaling efficacy depends on BcsA, DgcC and PdeK distance

The model has three unknown parameters: the diffusion coefficient D, the BcsA–DgcC–PdeK distance l and the reaction radius ρ. To test how the different parameters affect the signaling efficacy, we numerically simulated 10^4 trajectories from Eq. (1), performing a sensitivity analysis with regard to parameter choices of D, l and ρ and computed the hitting probabilities. As depicted in Figure 7(d), we find an inverse relationship between the reaction probability between c-di-GMP and BcsA and the distances of the local source (DgcC), target (BcsA) and sink (PdeK), which is in line with the notion of local signaling: the closer the source, target and sink are together, the more likely c-di-GMP is to interact with BcsA. This inverse relation is unaffected by the choice of realistic diffusion coefficients D. As shown in Figure 7(e), the reaction radius ρ has a scaling effect only: The larger the reaction radius, the larger the reaction probability. Hence, the simulations support the hypothesis that co-localization of DgcC and BcsA alone can increase signaling efficacy.

Cytosolic c-di-GMP does not contribute to BcsA binding

To estimate the relative contribution of cytosolic c-di-GMP on BcsA binding, we can make an argument based on the c-di-GMP concentration within a reaction volume around BcsA and how it is altered by local c-di-GMP production. Under physiological conditions, cytosolic c-di-GMP concentrations are quite low (approximately 1.3 pmol/mg total protein, corresponding to about 80 c-di-GMP molecules per cell), which is mainly due to high levels and activity of the c-di-GMP degrading enzyme PdeH [12]. Based on concentrations of cytosolic c-di-GMP, we can estimate the rate, and correspondingly the probability at which a cytosolic c-di-GMP molecule will react with BscA (for details, see the Mathematical Modeling section of the Supplementary Information). The same can be done for locally produced c-di-GMP. Comparing the two probabilities, we estimate that *cytosolic* c-di-GMP is approximately 750-fold less likely to interact with BcsA compared to a single *locally* produced c-di-GMP molecule (for detailed calculation, see Supplementary Information). In other words, a single locally produced c-di-GMP increases the interaction probability for BcsA about 750-fold.

Overall, our mathematical model thus suggests that a localized source of freely diffusible c-di-GMP is indeed able to efficiently and preferentially deliver c-di-GMP to a c-di-GMP-binding effector located in its immediate vicinity.

Discussion

High specificity of c-di-GMP signaling in the presence of many DGCs and PDEs

The surprising multiplicity of the enzymes that produce and degrade c-di-GMP combined to observations of high target specificities of particular DGCs and PDEs has puzzled researchers for years, and several explanations have been under discussion [2,58]. The simplest possibility to generate specificity seemed highly conditional expression or activity of different DGCs and PDEs. However, at least in *E. coli*, nearly all DGCs were found to be expressed and active at the same time [12]. Due to largely different K_d's for c-di-GMP binding, different c-di-GMP effectors may respond differentially to

conditionally different cellular c-di-GMP levels established by distinct DGCs and PDEs, a mechanism referred to as "global" c-di-GMP signaling [58,59]. In many cases, however, global cellular c-di-GMP levels do not correlate with the regulatory output of specific DGCs or PDEs [12,60,61]. This would be more consistent with "local" c-di-GMP signaling generating high specificity of c-di-GMP signaling pathways *via* direct protein–protein interactions between DGCs, PDEs and particular effector/target components [2,58]. A number of reports have indeed shown direct protein–protein interactions or specific cellular co-localization of distinct DGCs and/or PDEs with particular effector/target systems [12,13,62–68]. Notably, global and local c-di-GMP signaling as explanations for high DGC/PDE specificity of an effector/target process are not mutually exclusive. For instance, a relatively low global c-di-GMP concentration may be sufficient to serve an effector with a low K_d, while at the same time another effector with a high K_d may require a specific DGC operating right next to it, but also the latter effector may be served by an increased global c-di-GMP pool under some other conditions.

Local c-di-GMP signaling by direct interaction of DgcC and PdeK with the cellulose synthase complex

DgcC has long been known to be specifically required for activating cellulose biosynthesis [25,26] without affecting the very low cellular c-di-GMP pool in *E. coli* [12]. Here, we demonstrate that membrane-associated DgcC is an active DGC (Figure 2(b)), which binds to and co-purifies with the equally membrane-associated cellulose synthase complex (Figure 3). Direct interaction occurs between the membrane-intrinsic MASE2 domain of DgcC and the cellulose synthase BcsB subunit (Figure 4). Furthermore, DgcC was found to interact with PdeK, which is encoded by a gene right downstream from the cellulose synthase operon and which can also contact BcsB (Figure 4). Thus, DgcC and PdeK represent a functionally specialized DGC/PDE pair that can dock onto its specific effector/target system, the membrane-intrinsic cellulose synthase complex. Conceptually, this is similar to the biofilm-promoting interaction between the DGC GcbC and the transmembrane effector LapD in *Pseudomonas aeruginosa*. Upon binding c-di-GMP locally produced by GcbC, LapD sequesters a periplasmic protease (LapG), thereby preventing the latter from degrading the biofilm-promoting outer membrane adhesin LapA [66,67].

Protein–protein interactions in such local c-di-GMP signaling complexes may assume different roles [2]. On the one hand, *scaffolding* interactions would serve to just position a specific DGC or PDE as a local c-di-GMP source or sink, respectively, right next to a particular c-di-GMP binding effector/target system. On the other hand, protein–protein interactions within a multiprotein c-di-GMP signaling complex may also assume *regulatory* functions, i.e. directly activate or inhibit the molecular functions of the interacting proteins. In such a system, ongoing enzymatic activity can modulate the regulatory interactions, as described for the "trigger PDEs" PdeR and PdeL in *E. coli* [23]. Also the interaction of GcbC and LapD in *P. aeruginosa* (see above) has a regulatory impact, since GcbC on its own has very low DGC activity only, which is stimulated in the complex with its effector LapD and which is further enhanced when GcbC binds citrate as a small molecule signal ligand at its CACHE sensor domain [69]. By contrast, regulation of cellulose biosynthesis by DgcC and PdeK relies solely on their enzymatic activities, since single amino acid exchanges in their respective active centers eliminated their function in cellulose control entirely just as deletion mutations did (Figure 6(a)). Thus, cellulose synthase associated with DgcC and PdeK represents an example of local c-di-GMP signaling with scaffolding protein–protein interactions that establish a local c-di-GMP source and sink at a multiprotein complex.

DgcC and PdeK operate as local source and sink, respectively, in an open, non-compartmentalized mode of action

In principle, DgcC could either operate as a local, yet *open* source of high c-di-GMP giving rise to a dynamic local gradient of the signaling molecule or it could be part of a *closed* microcompartment with a DgcC-generated 'local pool' of c-di-GMP physically separated from the overall cellular pool. Our observation that the cellulose-negative phenotype of a non-functional A-site point mutation in DgcC (expressed at normal levels from a chromosomal $dgcC^{GGAAF}$ allele) can be compensated for by c-di-GMP synthesized by ectopically expressed other DGCs (Figure 6(b)) strongly argues against DgcC generating a locally confined pool of c-di-GMP to activate cellulose synthase. Rather, DgcC produces c-di-GMP in the immediate vicinity of cellulose synthase, with c-di-GMP in principle having three options: it may (i) bind to the PilZ domain of BcsA, (ii) bind and be degraded by the co-localized PdeK or (iii) diffuse away and be diluted into the very low global cellular pool of c-di-GMP. By contrast, an artificially increased cellular c-di-GMP pool due to extopic overexpression of other DGCs, can compensate for a lack of DgcC activity (Figure 6). These data also confirm again that DgcC specificity of activation of cellulose production is dependent on the very low c-di-GMP level, which in *E. coli* K-12 is maintained by high expression and activity of the "master PDE" PdeH [12].

As a theoretical support for our experimental results, we developed a minimal reaction–diffusion model to assess whether local production of c-di-GMP may specifically control cellulose synthase *via* BcsA binding. Our simulations showed that co-localization of DgcC and BcsA fosters c-di-GMP binding to BcsA by strongly increasing the hitting probability (Figure 7) at distances still several times larger than average diameters of globular proteins as those involved here [15,47,48,56]. The choice of different diffusion coefficients *D* had no effect on the hitting probability, and the reaction radius ρ had only a scaling influence. Additionally, we observed that "background" signaling by *cytosolic* c-di-GMP is negligible at physiological concentrations, but signaling is about 750-fold increased if a single c-di-GMP molecule is *locally* released by DgcC. Related mathematical approaches, e.g., analytical methods developed by Condamin *et al*. [70–72] can be used to assess the average time (mean first passage time [73,74]) until one molecule (BcsA) is hit by a freely diffusing other molecule (c-di-GMP). However, our objective here was to elucidate the dependence of a *reaction probability* on the source/target distance. For this purpose, the conducted simulation experiments already provided sufficiently insightful statistics.

It was previously shown that local production of c-di-GMP by DgcC does not alter the cytosolic c-di-GMP concentration, which is controlled by several active DGCs antagonized by the cytosolic master PDE PdeH (with the latter being present in up to 6000 molecules per cell) [12]. We did not explicitly consider *cytosolic* elimination of locally released c-di-GMP, but implicitly modeled it by assuming that locally released c-di-GMP is consumed when it leaves a certain radius around BcsA. On the other hand, we did not consider putative mechanisms that may retain c-di-GMP in proximity to its target. Thus, the estimated c-di-GMP-BcsA reaction probabilities may even under-predict the true reaction probability. Notably, the observed dependency of the reaction probability on the DgcC-BcsA distance would also hold if more complex simulation models were used. In the future, our simulation tool may incorporate yet undetermined additional biophysical and molecular parameters that allow to more accurately determine the binding probability of c-di-GMP to its target. This, in turn, may then be used to estimate the duration of target occupation and hence the requirements for local DgcC production. For example, the expected number of binding events for a single c-di-GMP molecule, considering re-binding, can be computed as E[binding events] = $p/(1-p)^2$, where p is the probability to bind BcsA, when c-di-GMP is produced/released at a specific distance l away from its target (akin to the parameter determined here in Figure 7(e)). Likewise, the expected duration of target occupation for a single produced c-di-GMP molecule is then E[duration of target occupation] = E[binding events]/k_{off}, where k_{off} is the rate at which c-di-GMP is released from BcsA.

Signal input and physiological role of local c-di-GMP control in cellulose biosynthesis

Localized action of DgcC and PdeK right next to the c-di-GMP binding site of cellulose synthase suggests that the activities of DgcC and PdeK may be differentially controlled to up- or down-regulate cellulose production. The transmembrane MASE2 domain of DgcC is a dimerization domain necessary for DGC activity of DgcC, which required us to reconstitute functional full-size protein in a lipid environment to detect activity *in vitro* (Figure 2(b)). No additional signal was necessary for DGC activity of this reconstituted DgcC, which could be an indication that dimerization of the N-terminal MASE2 domain does not need an activating signal. The K_m of DgcC (2 μM; Figure S4) is about 3 orders of magnitude lower than the cellular concentration of its substrate GTP [46], suggesting operation at its maximal rate. Also, in contrast to some other DGCs, DgcC shows only weak feedback inhibition by its own product (Figure 2(b)). Thus, DgcC may be mainly controlled at the level of transcription by the RpoS/MlrA/CsgD transcription factor cascade. On the other hand, the cytoplasmic part of PdeK alone, i.e. the GGDEF^{deg} domain linked to the canonical EAL domain, shows clear PDE activity *in vitro* (Figure 2(c)). Yet, the full-size PdeK protein seems to have little activity *in vivo* under our experimental conditions since complete deletion or point mutations in the active site generated weak phenotypes only (Figures 1 and 6(a)). This suggests that the membrane-inserted and periplasmic domains of PdeK could exert an inhibitory effect on its PDE activity. This inhibition may be counteracted, i.e. PdeK's role as a local c-di-GMP sink may be conditionally activated, by a still unknown signal or condition that physiologically requires cellulose synthesis to be rapidly shut down.

During entry into stationary phase, the production of curli fibers and cellulose production is *co-regulated via* the RpoS/MlrA/CsgD transcriptional cascade and the MlrA-activating input provided by the top level c-di-GMP module, which consists of DgcE, PdeR and DgcM [12,13,22]. What could be the physiological benefit of subjecting cellulose biosynthesis to a specific second layer of c-di-GMP control exerted locally by DgcC and PdeK? This additional c-di-GMP control of cellulose synthesis should allow cells to vary their curli:pEtN-cellulose production ratio. Thus, conditions that activate PdeK would shift this ratio in favor of curli fibers. On the other hand, DgcC-activated cellulose biosynthesis may continue, when CsgD, expressed in a transient burst during entry into stationary phase [12,75], is no longer produced and in fact has disappeared in stationary phase cells and thus no longer can activate curli gene expression. Different curli:pEtN-cellulose ratios are likely to affect the physical

properties of a biofilm, i.e. its elastic tissue-like behavior, since a curli-only matrix is brittle and tends to break, whereas cellulose, either alone or in a composite with curli fibers, as present in specific biofilm zones, confers matrix elasticity that allows buckling up and folding of *E. coli* macrocolony biofilms [16,30,31,76,77].

Conclusion and Perspectives

Local c-di-GMP signaling by DgcC and PdeK teaming up directly with cellulose synthase is highly specific, it allows cellulose biosynthesis to occur despite the low global cellular c-di-GMP level maintained by the master PDE PdeH, and it could provide for additional specific signal input. At the molecular level, it will be a future challenge to complement the currently known structure of the membrane-inserted BcsAB/BcsFG cellulose synthase/modification complex [27,47] with additional structures of DgcC in the active, i.e. dimeric form and of PdeK.

In more general terms, the example of DgcC and PdeK specifically controlling cellulose synthase also helps to define clear criteria, which should be met in combination to identify other cases of locally controlled c-di-GMP-binding effector/target systems in bacteria with multiple DGCs and PDEs: (1) a specific phenotype of a knockout of a particular DGC and/or PDE despite the presence and activity of other DGCs/PDEs; (2) no change of the global cellular c-di-GMP pool in these particular mutants; (3) an effector K_d for c-di-GMP binding that is several times higher than the actual global cellular c-di-GMP concentration under conditions of activation of the respective target process; and (4) direct interactions between the DGC, PDE and effector/target system. Notably, criterium 3 may apparently, but not factually be met in a situation of heterogeneity within a cellular population, where only a certain fraction of the cells may contain proportionately higher global cellular c-di-GMP levels and thus generate the relevant phenotype; in such a case, however, criterium 2 could not be met. Finally, we have demonstrated here experimentally and theoretically that local c-di-GMP signaling in bacteria can occur in open molecular systems; i.e. there is no need to postulate sequestration or subcellular compartimentalization.

Materials and Methods

Bacterial strains and growth conditions

Unless indicated otherwise, the strains used are derivatives of the *E. coli* K-12 strains W3110 [78] or AR3110, which is a direct derivative of W3110, in which codon 6 (the stop codon TAG) in the chromosomal copy of *bcsQ* was changed to the sense codon TTG, which rendered strain AR3110 cellulose-proficient [30]. *E. coli* strain 1094 and its $bcsA^{HA\text{-}Flag}$ 2 K7 derivative were previously described [47]. Knockout mutations in the W3110 or AR3110 backgrounds are full open reading frame deletion/antibiotic resistance cassette insertions previously described [11–13,18,30,79]. When required, cassettes were flipped out using the protocol of Datsenko and Wanner [80]. Mutations were transferred using P1 transduction [81]. The introduction of point mutations into chromosomal genes was performed with a two-step method related to the one-step gene inactivation [82]. Point mutations on plasmids were generated using a four-primer/two-step PCR protocol [83] and the oligonucleotide primers listed in Table S1.

Plasmids used for complementation, protein–protein interaction assays and protein overexpression and purification were constructed using oligonucleotide primers listed in Table S1. For *in vivo* two-hybrid assays, relevant genes or part of genes were cloned into pKT25, pKNT25, pUT18 or pUT18C (Euromedex), thereby generating fusion proteins with fragments of *B. pertussis* AC fused to the N terminus and C terminus of the relevant protein or domain. For pull-down experiments involving DgcC and for complementation assays, *dgcC*, *dgcE* and *dgcQ* full open-reading-frames were cloned into the $lacI^q$ *tac* promoter vector pCAB18Cm, which was generated from pCAB18 [84] by replacing the beta-lactamase gene (*bla*) by the chloramphenicol resistance gene (*cat*; primers are given in Table S1).

Cells were grown in liquid LB medium under aeration at 28 or 37 °C. Antibiotics were added as recommended [81]. Liquid culture growth was followed as optical density at 578 nm (OD_{578}).

Growth and stereomicroscopy of macrocolony biofilms

Growth of macrocolony biofilms was previously described [30,85]. Briefly, 5 µl of the overnight cultures (free of matrix, since grown in liquid LB at 37 °C) was spotted on salt-free LB agar plates. In order to achieve reproducible colony morphology, these plates always have to contain exactly the same volume of medium and have to be prepared under exactly identical conditions. In addition, all macrocolonies that had to be compared in a given experiment were grown on a single agar plate (up to 20 colonies can be grown on one plate when using 140-mm-diameter Petri dishes (VWR)). For the detection of CR binding (indicative of curli and pEtN-cellulose production), macrocolonies were grown on agar plates with salt-free LB or Yesca medium (casamino acids 10 g/l, yeast extract 1 g/l [86]) supplemented with CR and Coomassie brilliant blue (40 and 20 µg/ml, respectively). As an indicator of extracellular pEtN-cellulose, salt-free LB-plates were supplemented with Calcofluor Fluorescent Brightener 28 (100 µg/ml; Sigma) and Calcofluor-binding was detected using 366-nm UV-light (note that also curli fibers bind Calcofluor to some

extent; i.e. this assay is not strictly specific for pEtN-modified or unmodified cellulose). Since pEtN-cellulose and curli fiber expression occurs only below 30 °C in *E. coli* K-12 derivatives, cultures were grown at 28 °C unless otherwise indicated.

E. coli macrocolony biofilms were visualized at 10× magnification with a Stemi 2000-C stereomicroscope (Zeiss; Oberkochen, Germany). Digital images were captured with an AxioCamICC3 digital camera coupled to the stereomicroscope, operated *via* the AxioVision 4.8 software (Zeiss).

Bacterial two-hybrid analysis for testing protein–protein interactions *in vivo*

To test for specific protein–protein interactions, a bacterial two-hybrid system based on the restoration of cAMP-signaling in a *Δcya* mutant was used [40]. Oligonucleotide primers for generating the W3110 *Δcya* mutant and for the cloning of sequences encoding full-size proteins or domains onto pUT18/pUT18C and pKT25/pKNT25 plasmids to generate fusion-proteins are listed in the Supplementary Information. Plasmids were co-transformed into the *Δcya* mutant and incubated on MacConkey agar plates supplemented with lactose (1%), ampicillin (100 µg/ml) and kanamycin (50 µg/ml) for 30 h at 28 °C. Red colonies indicate utilization of lactose, which depends on cAMP production due to direct interaction of the proteins fused to the otherwise separate AC domains. All colonies to be compared were grown together on a single agar plate (140-mm diameter), but separate close-up photographs were taken.

Protein overexpression and purification

pETDuet1-based plasmids were transformed into *E. coli* ER2556 (New England Biolabs; for expressing PdeK$^{aa148–649}$::Strep) or *E. coli* C41 pRARE2 (for expressing DgcC::Strep). Cells were grown in LB or TB [81] supplemented with 100 µg/ml ampicillin and/or 15 µg/ml chloramphenicol until an OD_{578} of 0.5–0.8, and protein expression was induced using 0.1 mM IPTG.

For the purification of soluble PdeK$^{aa148–649}$::Strep, IPTG-induced LB-cultures were incubated for 4 h at 28 °C. Cells were harvested by centrifugation and stored at −80 °C until further use. For protein purification, cell pellets were resuspended in 50 mM Tris (pH 8.0), 10 mM $MgCl_2$, 300–500 mM NaCl, 1 mM EDTA and 0.5 mM PMSF. Cells were disrupted by two passages through a French press, and cell debris were removed by centrifugation for 40 min at 19,000 rpm in a SS-34 rotor at 4 °C. The supernatant was incubated under gentle shaking overnight with Strep-Tactin Sepharose (Iba) matrix (2.5 ml per 500 ml cell culture) at 4 °C. The resin was washed using the resuspension buffer mentioned above supplemented with 20–40 mM imidazole and Strep-tagged protein was eluted using Strep-Tactin Elution buffer (Iba). Before storage at −80 °C, the purified proteins were dialyzed against PDE Reaction Buffer (see below).

For the purification of the membrane-associated DgcC::Strep, IPTG-induced TB-cultures were incubated for 5 h at 37 °C. Cells were harvested by centrifugation and stored at −80 °C until further use. For protein purification, cell pellets were resuspended in 50 mM Tris (pH 8.0), 10 mM $MgCl_2$ 300 mM NaCl, 1 mM EDTA, 0.5 mM PMSF and protease inhibitor cocktail (complete, EDTA-free; Roche), and cells were disrupted by two passages through a French press. Intact cells were removed by centrifugation for 20 min at 5000 rpm, and total membranes were collected by ultra-centrifugation for 1 h at 36,000 rpm (T647.5 rotor). The membrane pellet was solubilized in 50 mM Tris (pH 8.0), 10 mM $MgCl_2$ 300 mM NaCl, 5% glycerol, 2% dodecyl-β-D-maltosid (Roth), 1 mM EDTA and 0.5 mM PMSF for 2 h at 4 °C. Solubilized and non-solubilized proteins were separated by a second ultra-centrifugation step. The supernatant was incubated with or Strep-Tactin Sepharose (1 ml added to the supernatant obtained from 2000 ml of cell culture) overnight at 4 °C. The resin was washed using solubilization buffer supplemented with 0.05% DDM. Proteins were eluted using Strep-Tactin Elution buffer (Iba) also supplemented with 0.05% DDM. Glycerol was added to the eluted proteins to a final concentration of 10%, and samples were stored at −80 °C until further use.

Expression and purification of MSP was performed as described previously [45]. MSP1E3D1 was overexpressed in *E. coli* BL21(DE3). Purification and TEV-protease digestion were performed in co-operation with Prof. Erwin Schneider, Humboldt-Universität zu Berlin.

Expression and purification of PleD* was as described [42].

Reconstitution of DgcC into lipid bilayer nanodiscs

The reconstitution of DgcC-Strep into nanodiscs was performed as previously described [87]. Briefly, 8.3 mg of chloroform solubilized *E. coli* total lipid extract (Avanti Polar Lipids) was vacuum dried. Lipids were subsequently hydrated by the addition of 0.9 ml ND buffer (20 mM Tris (pH 7.5), 100 mM NaCl), 87 µl 10% DDM and 5–10 min of sonification. Purified MSP1E3D1 (1.62 mg) and 0.8 mg purified DgcC-Strep (for purification procedure, see above) were added to the lipids, resulting in a molar ratio of 7:2. Samples were incubated for 1 h at 4 °C, and the detergent was removed using 1.5 g wet SM-2 Biobeads (Biorad, equilibrated in ND buffer) per 5 ml volume. As the membrane-protein-storage buffer contains 10% glycerol, which interferes with nanodisc-formation, ND buffer was added until glycerol concentration decreased below 3%. To prevent lipid oxidation, samples were covered with N_2 gas. After 4 h of incubation at 4 °C, ND-buffer

containing the nanodiscs was separated from the beads and incubated with Strep-Tactin Sepharose overnight. Purification of nanodiscs with incorporated DgcC-Strep was performed as described for purification of DgcC-protein except for the absence of detergent and protease inhibitor. Approximately equal concentrations of the scaffold protein and DgcC in the nanodiscs (two molecules of each should be present per nanodisc) were controlled by SDS polyacrylamide gel electrophoresis. Eluates containing DgcC-Strep nanodiscs were stored at 4 °C no longer than 3 days.

Determination of DGC and PDE activities with purified and reconstituted proteins *in vitro*

DGC and PDE reactions were performed with purified cytoplasmic proteins or membrane protein complexes incorporated into nanodiscs. Activities were assayed with [P^{33}]-GTP and [P^{33}]-c-di-GMP as substrates, respectively, following standard procedures [42,79,88]. PDE-reaction buffer contained 25 mM Tris (pH 8.0), 100 mM NaCl, 10 mM $MgCl_2$, 5 mM β-mercaptoethanol and 5% glycerol. DGC-reaction buffer used for DgcC-nanodiscs contained 25 mM Tris (pH 7.5), 100 mM NaCl; 5 mM $MgCl_2$ or other cations (as chloride salts) as indicated and 2.5 mM β-mercaptoethanol. Proteins were used at a molar concentration up to 4 μM and were incubated with [P^{33}]-GTP (3000 Ci/mmol; 82.5 or 41 nM for standard DGC assays and K_m(GTP) determinations, respectively) or [P^{33}]-c-di-GMP (3000 Ci/mmol; 82.5 nM, for PDE assay; all radiolabeled compounds obtained from Hartmann Analytic GmbH). Samples were incubated at 30 °C, and the reaction was stopped by adding a similar volume of EDTA (final concentration 250 mM) after the indicated time points. Reaction products were separated by thin layer chromatography (cellulose-coated TLC-plate, Machery-Nagel; TLC-buffer: saturated NH_4SO_4 and 1.5 M KH_2PO_4 at a 2:3 ratio) and quantified by phosphor imaging and the ImageQuant TL Array Analysis v8.1 software.

Detection of direct interactions between DgcC and the cellulose synthase complex by affinity chromatography

DgcC with C-terminal His6 tag was expressed from the pCAB18 vector in the *E. coli* 1094 or 1094 *bcsA*$^{HA\text{-}Flag}$ 2 K7 strains. Membrane fractions were prepared as previously described by Krasteva *et al.* [47] with minor changes, using dodecyl-β-D-maltosid (2% for solubilization at 4 °C for 3 h and 0.05% for washing and elution, respectively) instead of Triton X-100 and a modified buffer A (20 mM Tris (pH 7.5), 150 mM NaCl, 7% glycerol and 10 mM $MgCl_2$). Solubilized membrane fractions were incubated with anti-FlagM2 affinity gel (Sigma/Merck) overnight at 4 °C in a rotating mixer and elution was performed with 3× FLAG peptide (Sigma/Merck). Proteins were detected by SDS-PAGE and immunoblotting.

SDS polyacrylamide gelelectrophoresis and immunoblotting

Proteins were detected by SDS polyacrylamide gel electrophoresis (SDS-PAGE) and immunoblotting as previously described [89] using antibodies against the Flag tag (Sigma) or the 6His-tag (Bethyl Laboratories, Inc.) at 1:10,000 dilution. Anti-rabbit or anti-mouse IgG alkaline phosphatase conjugate from goat (Sigma) was used (at 1:10000 dilution) and for signal detection incubated with NBT/BCIP in alkaline phosphatase buffer. The WesternSure® Pre-stained Chemiluminescent Protein Ladder (Li-cor) was used as a molecular mass standard.

Determination of cellular c-di-GMP levels

Strains were grown at 28 °C under aeration in LB medium. At an OD_{578} of 3, 10 ml culture volume was pelleted (4 °C, 5000 rpm, 30 min) and stored at −80 °C. Sample extraction and analysis of c-di-GMP by LC–MS/MS was performed as described previously [90]. Intracellular concentrations of c-di-GMP were calculated by using the standard OD/cell mass ratio [81]. Extractions were performed in biological triplicates.

Determination of β-galactosidase activity

β-Galactosidase activity was assayed by use of *o*-nitrophenyl-β-D-galactopyranoside as a substrate and is reported as mmol of *o*-nitrophenol per min per mg of cellular protein [81].

Biological replicates and statistics of experiments

All experiments shown in this study were done at least three times as independent, i.e. biological replicates. Photographic documentation of representative experimental results is shown. In experiments generating single data points, figures show the average of three biological replicates with standard deviations given. Experiments showing the expression of *lacZ* fusions along the entire growth cycle were done at least three times, and a representative experiment is shown.

Acknowledgments

We thank Erwin Schneider and Heidi Landmesser (Humboldt-Universität zu Berlin) for providing purified MSP and helpful advice in nanodisc preparation. We

are grateful to Jean-Marc Ghigo (Institut Pasteur, Paris) for providing *E. coli* strains 1094 and its $bcsA^{HA\text{-}Flag}$ 2 K7 derivative.

This work was supported by the European Research Council under the European Union's Seventh Framework Programme (ERC-AdG 249780) and Deutsche Forschungsgemeinschaft (DFG grants He1556/17-1; He1556/21-1 as part of DFG Priority Programme 1879 "Nucleotide Second Messenger Signaling in Bacteria"), with these grants awarded to R.H.; and by the German Federal Ministry for Education and Research (BMBF; grant number 031A307) with this grant awarded to M.v.K.

Author Contributions

Concept of the study: R.H.; design of experiments: A.M.R., A.P., R.H.; wet lab experiments: A.M.R., A. P., S.H.; interpretation of experimental data: A.M.R., A.P., S.H., R.H.; mathematical modeling: N.M., K.P. Y., M.v.K.; writing of the paper: R.H. with input from the other authors.

Appendix A. Supplementary data

Supplementary data to this article can be found online at https://doi.org/10.1016/j.jmb.2020.06.006.

Received 16 December 2019;
Received in revised form 20 May 2020;
Accepted 8 June 2020
Available online 11 June 2020

Keywords:
bacterial second messenger;
cellulose synthase;
diguanylate cyclase;
GGDEF domain

Abbreviations used:
DGC, diguanylate cyclase; PDE, phosphodiesterase; c-di-GMP, bis-(3′–5′)-cyclic diguanosine monophosphate; pEtN, phosphoethanolamine; CR, Congo red; AC, adenylate cyclase; MSP, membrane scaffold protein.

References

[1] Jenal, U., Malone, J., (2006). Mechanisms of cyclic-di-GMP signaling in bacteria. *Annu. Rev. Genet.*, **40**, 385–407.
[2] Hengge, R., (2009). Principles of cyclic-di-GMP signaling. *Nat. Rev. Microbiol.*, **7**, 263–273.
[3] Römling, U., Galperin, M.Y., Gomelsky, M., (2013). Cyclic-di-GMP: the first 25 years of a universal bacterial second messenger. *Microbiol. Mol. Biol. Rev.*, **77**, 1–52.
[4] Jenal, U., Reinders, A., Lori, C., (2017). Cyclic-di-GMP: second messenger extraordinaire. *Nat. Rev. Microbiol.*, **15**, 271–284.
[5] Hengge, R., (2010). Role of c-di-GMP in the regulatory networks of *Escherichia coli*. in: A.J. Wolfe, K.L. Visick (Eds.), The Second Messenger Cyclic-Di-GMP, ASM Press, Washington, DC 2010, pp. 230–252.
[6] Hengge, R., Gründling, A., Jenal, U., Ryan, R.P., Yildiz, F.H., (2015). Bacterial signal transduction by c-di-GMP and other nucleotide second messengers. *J. Bacteriol.*, **198**, 15–26.
[7] Povolotsky, T.L., Hengge, R., (2016). Genome-based comparison of c-di-GMP signaling in commensal and pathogenic *Escherichia coli*. *J. Bacteriol.*, **198**, 111–126.
[8] Suzuki, K., Babitzke, P., Kushner, S.R., Romeo, T., (2006). Identification of a novel regulatory protein (CsrD) that targets the global regulatory RNAs CsrB and CsrC for degradation by RNase E. *Genes Dev.*, **20**, 2605–2617.
[9] Takaya, A., Erhardt, M., Karata, K., Winterberg, K., Yamamoto, T., Hughes, K.T., (2012). YdiV: a dual function protein that targets FlhDC for ClpXP-dependent degradation by promoting release of DNA-bound FlhDC complex. *Mol. Microbiol.*, **83**, 1268–1284.
[10] Tschowri, N., Busse, S., Hengge, R., (2009). The BLUF-EAL protein YcgF acts as a direct anti-repressor in a blue light response of *E. coli*. *Genes Dev.*, **23**, 522–534.
[11] Sommerfeldt, N., Possling, A., Becker, G., Pesavento, C., Tschowri, N., Hengge, R., (2009). Gene expression patterns and differential input into curli fimbriae regulation of all GGDEF/EAL domain proteins in *Escherichia coli*. *Microbiology*, **155**, 1318–1331.
[12] Sarenko, O., Klauck, G., Wilke, F.M., Pfiffer, V., Richter, A.M., Herbst, S., Kaever, V., Hengge, R., (2017). More than enzymes that make and break c-di-GMP—the protein interaction network of GGDEF/EAL domain proteins of *Escherichia coli*. *mBio*, **8**, e01639-17.
[13] Lindenberg, S., Klauck, G., Pesavento, C., Klauck, E., Hengge, R., (2013). The EAL domain phosphodiesterase YciR acts as a trigger enzyme in a c-di-GMP signaling cascade in *E. coli* biofilm control. *EMBO J.*, **32**, 2001–2014.
[14] Amikam, D., Galperin, M.Y., (2006). PilZ domain is part of the bacterial c-di-GMP binding protein. *Bioinformatics*, **22**, 3–6.
[15] Morgan, J.L., McNamara, J.T., Zimmer, J., (2014). Mechanism of activation of bacterial cellulose synthase by cyclic di-GMP. *Nat. Struct. Mol. Biol.*, **21**, 489–496.
[16] Thongsomboon, W., Serra, D.O., Possling, A., Hadjineophytou, C., Hengge, R., Cegelski, L., (2018). Phosphoethanolamine cellulose: a naturally produced chemically modified cellulose. *Science*, **359**, 334–338.
[17] Steiner, S., Lori, C., Boehm, A., Jenal, U., (2013). Allosteric activation of exopolysaccharide synthesis through cyclic di-GMP-stimulated protein–protein interaction. *EMBO J.*, **32**, 354–368.
[18] Pesavento, C., Becker, G., Sommerfeldt, N., Possling, A., Tschowri, N., Mehlis, A., Hengge, R., (2008). Inverse regulatory coordination of motility and curli-mediated adhesion in *Escherichia coli*. *Genes Dev.*, **22**, 2434–2446.
[19] Boehm, A., Kaiser, M., Li, H., Spangler, C., C.A., K., Ackerman, M., Kaever, V., Sourjik, V., et al., (2010). Second messenger-mediated adjustment of bacterial swimming velocity. *Cell*, **141**, 107–116.
[20] Fang, X., Gomelsky, M., (2010). A post-translational, c-di-GMP-dependent mechanism regulating flagellar motility. *Mol. Microbiol.*, **76**, 1295–1305.
[21] Paul, K., Nieto, V., Carlquist, W.C., Blair, D.F., Harshey, R. M., (2010). The c-di-GMP binding protein YcgR controls flagellar motor direction and speed to affect chemotaxis by a "backstop brake" mechanism. *Mol. Cell*, **38**, 128–139.

[22] Pfiffer, V., Sarenko, O., Possling, A., Hengge, R., (2019). Genetic dissection of *Escherichia coli*'s master diguanylate cyclase DgcE: role of the N-terminal MASE1 domain and direct signal input from a GTPase partner system. *PLoS Genet.*, **15**, e1008059.
[23] Hengge, R., (2016). Trigger phosphodiesterases as a novel class of c-di-GMP effector proteins. *Philos. Trans. R. Soc. B*, **371**, 20150498.
[24] Serra, D.O., Hengge, R., (2019). A c-di-GMP-based switch controls local heterogeneity of extracellular matrix synthesis which is crucial for integrity and morphogenesis of *Escherichia coli* macrocolony biofilms. *J. Mol. Biol.*, **431**, 4775–4793.
[25] Zogaj, X., Nimtz, M., Rohde, M., Bokranz, W., Römling, U., (2001). The multicellular morphotypes of *Salmonella typhimurium* and *Escherichia coli* produce cellulose as the second component of the extracellular matrix. *Mol. Microbiol.*, **39**, 1452–1463.
[26] Brombacher, E., Baratto, A., Dorel, C., Landini, P., (2006). Gene expression regulation by the curli activtor CsgD protein: modulation of cellulose biosynthesis and control of negative determinants for microbial adhesion. *J. Bacteriol.*, **188**, 2027–2037.
[27] McNamara, J.T., Morgan, J.L., Zimmer, J., (2015). A molecular description of cellulose biosynthesis. *Annu. Rev. Biochem.*, **84**, 895–921.
[28] Flemming, H.-C., Wingender, J., (2010). The biofilm matrix. *Nat. Rev. Microbiol.*, **8**, 623–633.
[29] Hufnagel, D.A., DePas, W.H., Chapman, M., (2015). The biology of the *Escherichia coli* extracellular matrix. *Microbiol. Spectrum*, **3**, MB-0014-2014.
[30] Serra, D.O., Richter, A.M., Hengge, R., (2013). Cellulose as an architectural element in spatially structured *Escherichia coli* biofilms. *J. Bacteriol.*, **195**, 5540–5554.
[31] Serra, D.O., Richter, A.M., Klauck, G., Mika, F., Hengge, R., (2013). Microanatomy at cellular resolution and spatial order of physiological differentiation in a bacterial biofilm. *mBio*, **4**, (2) e00103-13.
[32] Serra, D.O., Klauck, G., Hengge, R., (2015). Vertical stratification of matrix production is essential for physical integrity and architecture of macrocolony biofilms of *Escherichia coli*. *Environ. Microbiol.*, **17**, 5073–5088.
[33] Hengge, R., (2020). Linking bacterial growth, survival and multicellularity—small signaling molecules as triggers and drivers. *Curr. Opin. Microbiol.*, (2020) https://doi.org/10.1016/j.mib.2020.02.007 Epub 2020 Mar 31.
[34] Christen, B., Christen, M., Paul, R., Schmid, F., Folcher, M., Jenoe, P., Meuwly, M., Jenal, U., (2006). Allosteric control of cyclic di-GMP signaling. *J. Biol. Chem.*, **281**, 32015–32024.
[35] Rao, F., Yang, Y., Qi, Y., Liang, Z.X., (2008). Catalytic mechanism of c-di-GMP specific phosphodiesterase: a study of the EAL domain-containing RocR from *Pseudomonas aeruginosa*. *J. Bacteriol.*, **190**, 3622–3631.
[36] Tchigvintsev, A., Xu, X., Singer, A., Chang, C., Brown, G., Proudfoot, M., Cui, H., Flick, R., et al., (2010). Structural insight into the mechansm of c-di-GMP hydrolysis by EAL domain phosphodiesterases. *J. Mol. Biol.*, **402**, 524–538.
[37] Robert-Paganin, J., Nonin-Lecomte, S., Réty, S., (2012). Crystal structure of an EAL domain in complex with reaction product 5′-pGpG. *PLoS One*, **7**, e52424.
[38] Grigorenko, B.L., Knyazeva, M.A., Nemukhin, A.V., (2016). Analysis of proton wires in the enzyme active site suggests a mechanism of c-di-GMP hydrolysis by the EAL domain phosphodiesterases. *Proteins*, **84**, 1670–1680.
[39] Nikolskaya, A.N., Mulkidjanian, A.Y., Beech, I.B., Galperin, M.Y., (2003). MASE1 and MASE2: two novel integral membrane sensory domains. *J. Mol. Microbiol. Biotechnol.*, **5**, 11–16.
[40] Karimova, G., Pidoux, J., Ullmann, A., Ladant, D., (1998). A bacterial two-hybrid system based on a reconstituted signal transduction pathway. *Proc. Natl. Acad. Sci. U. S. A.*, **95**, 5752–5756.
[41] Chan, C., Paul, R., Samoray, D., Amiot, N., Giese, B., Jenal, U., Schirmer, T., (2004). Structural basis of activity and allosteric control of diguanylate cyclase. *Proc. Natl. Acad. Sci. U. S. A.*, **101**, 17084–17089.
[42] Paul, R., Weiser, S., Amiot, N., Chan, C., Schirmer, T., Giese, B., Jenal, U., (2004). Cell cycle-dependent dynamic localization of a bacterial response regulator with a novel di-guanylate cyclase output domain. *Genes Dev.*, **18**, 715–727.
[43] Bayburt, T.H., Grinkova, Y.V., Sligar, S.G., (2002). Self-assembly of discoidal phospholipid bilayer nanoparticles with membrane scaffold proteins. *Nano Lett.*, **2**, 853–856.
[44] Borch, J., Hamann, T., (2009). The nanodisc: a novel tool for membrane protein studies. *Biol. Chem.*, **390**, 805–814.
[45] Ritchie, T.K., Grinkova, Y.V., Bayburt, T.H., Denisov, I.G., Zolnerciks, J.K., Atkins, W.M., Sligar, S.G., (2009). Chapter 11—reconstitution of membrane proteins in phospholipid nanodiscs. *Methods Enzymol.*, **464**, 211–231.
[46] Buckstein, M.H., He, J., Rubin, H., (2008). Characterization of nucleotide pools as a function of physiological state in *Escherichia coli*. *J. Bacteriol.*, **190**, 718–726.
[47] Krasteva, P.V., Bernal-Bayard, J., Travier, L., Martin, F.A., Kaminski, P.A., Karimova, G., Fronzes, R., Ghigo, J.-M., (2017). Insights into the structure and assembly of a bacterial cellulose secretion system. *Nat. Commun.*, **8**, 2065.
[48] Morgan, J.L.W., Strumillo, J., Zimmer, J., (2013). Crystallographic snapshot of cellulose synthesis and membrane translocation. *Nature*, **493**, 181–186.
[49] Barends, T.R., Hartmann, E., Griese, J.J., Beitlich, T., Kirienko, N.V., Ryjenkov, D.A., Reinstein, J., Shoeman, R.L., et al., (2009). Structure and mechanism of a bacterial light-regulated cyclic nucleotide phosphodiesterase. *Nature*, **18**, 1015–1018.
[50] Sundriyal, A., Massa, C., Samoray, D., Zehender, F., Sharpe, T., Jenal, U., Schirmer, T., (2014). Inherent regulation of EAL domain-catalyzed hydrolysis of second messenger cyclic di-GMP. *J. Biol. Chem.*, **289**, 6978–6990.
[51] Erban, R., Chapman, S.J., (2009). Stochastic modelling of reaction-diffusion processes: algorithms for bimolecular reactions. *Phys. Biol.*, **6**, 046001.
[52] Lamba, H., Mattingly, J.C., Stuart, M., (2007). An adaptive Euler–Maruyama scheme for SDSs: convergence and stability. *IMA J. Num. Anal.*, **27**, 479–506.
[53] Kloeden, P.E., Platen, E., (1992). Numerical Solution of Stochastic Differential Equations. Springer, Berlin Heidelberg, 1992.
[54] Olson, A., Pugh Jr. Jr., E.N., (1993). Diffusion coefficient of cyclic GMP in salamander rod outer segments estimated with two fluorescent probes. *Biophys. J.*, **65**, 1335–1352.
[55] Zhou, J., Sayre, D.A., Wang, J., Pahadi, N., Sintim, H.O., (2012). Endo-S-c-di-GMP analogues—polymorphism and binding studies with class I riboswitch. *Molecules*, **17**, 13376–13389.
[56] Schirmer, T., Jenal, U., (2009). Structural and mechanistic determinants of c-di-GMP signalling. *Nat. Rev. Microbiol.*, **7**, 724–735.
[57] Erickson, H.P., (2009). Size and shape of protein molecules at the nanometer level determined by

sedimentation, gel filtration, and electron microscopy. *Biol. Proced. Online*, **11**, 32–51.
[58] Dahlström, K.M., O'Toole, G.A., (2017). A symphony of cyclases: specificity in diguanylate cyclase signaling. *Annu. Rev. Microbiol.*, **71**, 179–195.
[59] Pultz, I.S., Christen, M., Kulasakara, H.D., Kennard, A., Kulasakara, B.R., Miller, S.I., (2012). The response threshold of *Salmonella* PilZ domain proteins is determined by their binding affinities for c-di-GMP. *Mol. Microbiol.*, **86**, 1424–1440.
[60] Merritt, J.H., Ha, D.-G., Cowles, K.N., Lu, W., Morales, D.K., Rabinowitz, J., Gitai, Z., O'Toole, G.A., (2010). Specific control of *Pseudomonas aeruginosa* surface-associated behaviours by two c-di-GMP diguanylate cyclases. *mBio*, **1**, e00183-10.
[61] Massie, J.P., Reynolds, E.L., Koestler, B., Cong, J.-P., Agostoni, M., Waters, C.M., (2012). Quantification of high-specificity cyclic diguanylate signaling. *Proc. Natl. Acad. Sci. U. S. A.*, **109**, 12746–12751.
[62] Abel, S., Chien, P., Wassmann, P., Schirmer, T., Kaever, V., Laub, M.T., Baker, T.A., Jenal, U., (2011). Regulatory cohesion of cell cycle and cell differentiation through interlinked phosphorylation and second messenger networks. *Mol. Cell*, **43**, 550–560.
[63] Andrade, M.O., Alegria, M.C., Guzzo, C.R., Docena, C., Rosa, M.C., Ramos, C.H., Farah, C.S., (2006). The HD-GYP domain of RpfG mediates a direct linkage between the Rpf quorum-sensing pathway and a subset of diguanylate cyclase proteins in the phytopathogen *Xanthomonas axonopodis* pv citri. *Mol. Microbiol.*, **62**, 537–551.
[64] Bobrov, A.G., Kirillina, O., Forman, S., Mack, D., Perry, R.D., (2008). Insights into *Yersinia pestis* biofilm development: topology and co-interaction of Hms inner membrane proteins involved in exopolysaccharide production. *Environ. Microbiol.*, **10**, 1419–1432.
[65] Tuckerman, J.R., Gonzalez, G., Gilles-Gonzalez, M.-A., (2011). Cyclic di-GMP activation of polynucleotide phosphorylase signal-dependent RNA processing. *J. Mol. Biol.*, **407**, 633–639.
[66] Dahlström, K.M., Giglio, K.M., Collins, A.J., Sondermann, H., O'Toole, G.A., (2015). Contribution of physical interactions to signaling specificity between a diguanylate cyclase and its effector. *mBio*, **6**, e01978-15.
[67] Dahlström, K.M., Giglio, K.M., Sondermann, H., O'Toole, G.A., (2016). The inhibitory site of a diguanylate cyclase is a necessary element for interaction and signaling with an effector protein. *J. Bacteriol.*, **198**, 1595–1603.
[68] Valentini, M., Laventie, B.-J., Moscoso, J., Jenal, U., Filloux, A., (2016). The diguanylate cyclase HsbD itersects with the HptB regulatory cascade to control *Pseudomonas aeruginosa* biofilm and motility. *PLoS Genet.*, **12**, e1006354.
[69] Giacalone, D., Smith, T.J., Collins, A.J., Sondermann, H., Koziol, L.J., O'Toole, G.A., (2018). Ligand-mediated biofilm formation via enhanced physical interaction between a diguanylate cyclase and its receptor. *mBio*, **9**, e01254-18.
[70] Condamin, S., Bénichou, O., Moreau, M., (2005). First-passage times for random walks in bounded domains. *Phys. Rev. Lett.*, **95**, 260601.
[71] Condamin, S., Bénichou, O., Klafter, J., (2007). First-passage time distributions for subdiffusion in confined geometry. *Phys. Rev. Lett.*, **98**, 250602.
[72] Condamin, S., Bénichou, O., Tejedor, V., Voituriez, R., Klafter, J., (2007). First-passage times in complex scale-invariant media. *Nature*, **450**, 77–80.
[73] Mattos, T.G., Mejía-Monasterio, C., Metzler, R., Oshanin, G., Schehr, G., (2014). Trajectory to trajectory fluctuations in first-passage phenomena in bounded domains. in: R. Metzler, G. Oshanin, S. Redner (Eds.), First-Passage Phenomena and Their Applications, World Scientific Publishing, Singapore 2014, pp. 203–225.
[74] Mejía-Monasterio, C., Oshanin, G., Schehr, G., (2011). First passages for a search by a swarm of independent random searchers. *J. Statist. Mechan. Theory Exp.*, P06022.
[75] Mika, F., Busse, S., Possling, A., Berkholz, J., Tschowri, N., Sommerfeldt, N., Pruteanu, M., Hengge, R., (2012). Targeting of *csgD* by the small regulatory RNA RprA links stationary phase, biofilm formation and cell envelope stress in *Escherichia coli*. *Mol. Microbiol.*, **84**, 51–65.
[76] Serra, D.O., Hengge, R., (2014). Stress responses go three-dimensional—the spatial order of physiological differentiation in bacterial macrocolony biofilms. *Environ. Microbiol.*, **16**, 1455–1471.
[77] Klauck, G., Serra, D.O., Possling, A., Hengge, R., (2018). Spatial organization of different sigma factor activities and c-di-GMP signalling within the three-dimensional landscape of a bacterial biofilm. *Open Biol.*, **8**, 180066.
[78] Hayashi, K., Morooka, N., Yamamoto, Y., Fujita, K., Isono, K., Choi, S., Ohtsubo, E., Baba, T., et al., (2006). Highly accurate genome sequences of *Escherichia coli* K-12 strains MG1655 and W3110. *Mol. Syst. Biol.*, **2**, 2006.0007.
[79] Weber, H., Pesavento, C., Possling, A., Tischendorf, G., Hengge, R., (2006). Cyclic-di-GMP-mediated signaling within the σ^S network of *Escherichia coli*. *Mol. Microbiol.*, **62**, 1014–1034.
[80] Datsenko, K.A., Wanner, B.L., (2000). One-step inactivation of chromosomal genes in *Escherichia coli* K-12 using PCR products. *Proc. Natl. Acad. Sci. U. S. A.*, **97**, 6640–6645.
[81] Miller, J.H., (1972). Experiments in Molecular Genetics. Cold Spring Harbor Laboratory, Cold Spring Harbor, NY, 1972.
[82] Kolmsee, T., Hengge, R., (2011). Rare codons play a positive role in the expression of the stationary phase sigma factor RpoS (σ^S) in *Escherichia coli*. *RNA Biol.*, **8**, 913–921.
[83] Germer, J., Becker, G., Metzner, M., Hengge-Aronis, R., (2001). Role of activator site position and a distal UP-element half-site for sigma factor selectivity at a CRP/H-NS activated σ^S-dependent promoter in *Escherichia coli*. *Mol. Microbiol.*, **41**, 705–716.
[84] Barembruch, C., Hengge, R., (2007). Cellular levels and activity of the flagellar sigma factor FliA of *Escherichia coli* are controlled by FlgM-modulated proteolysis. *Mol. Microbiol.*, **65**, 76–89.
[85] Serra, D.O., Hengge, R., (2017). Experimental detection and visualization of the extracellular matrix in macrocolony biofilms. in: K. Sauer (Ed.), C-Di-GMP Signaling: Methods & Protocols—Methods in Molecular Biology, Humana Press, Springer Nature, New York, NY 2017, pp. 133–145.
[86] DePas, W.H., Hufnagel, D.A., Lee, J.S., Blanco, L.P., Bernstein, H.C., Fisher, S.T., James, G.A., Stewart, P.S., et al., (2013). Iron induces bimodal population development by *Escherichia coli*. *Proc. Natl. Acad. Sci. U. S. A.*, **110**, 2629–2634.
[87] Herbst, S., Lorkowski, M., Sarenko, O., Nguyen, T.K. L., Jaenicke, T., Hengge, R., (2018). Transmembrane redox and proteolysis control of c-di-GMP signaling in bacterial biofilm formation. *EMBO J.*, **37**, e97825.

[88] Christen, M., Christen, B., Folcher, M., Schauerte, A., Jenal, U., (2005). Identification and characterization of a cyclic di-GMP-specific phosphodiesterase and its allosteric control by GTP. *J. Biol. Chem.*, **280**, 30829–30837.

[89] Lange, R., Hengge-Aronis, R., (1994). The cellular concentration of the σ^S subunit of RNA-polymerase in *Escherichia coli* is controlled at the levels of transcription, translation and protein stability. *Genes Dev.*, **8**, 1600–1612.

[90] Spangler, C., Böhm, A., Jenal, U., Seifert, R., Kaever, V., (2010). A liquid chromatography-coupled tandem mass spectrometry method for quantitation of cyclic-di-guanosine monophosphat. *J. Microbiol. Methods*, **81**, 226–231.